

### Chapter 3

*An assessment of the paleoecological implications of terrestrial gastropods  
from western Wisconsin using Amino Acid Racemization*

#### ABSTRACT

Many important questions in paleoecological studies rely upon the temporal fidelity of a fossil deposit. The amino acid composition of 236 terrestrial gastropod shells from two late Pleistocene fossil localities in western Wisconsin (Big Platte and Kulas Quarry) was measured using HPLC. Four amino acids (aspartic acid, glutamic acid, serine, and alanine) were analyzed for their total concentration and D/L values.  $^{14}\text{C}$  dates from succineid shells at these sites indicated a full-glacial age for the assemblage (ca. 22,000 – 18,000 cal yr BP). Cordilleran-Boreal taxa (*Succinea*, *Catinella*, *Discus*, *Vertigo*, *Columella*, *Pupilla*, and *Vallonia*) had more weathered shells and D/L Asp values from 0.300 to 0.350, characteristic of late Pleistocene ages. The less weathered shells of rare Eastern Deciduous Forest taxa (*Helicodiscus*, *Hawaiiia*, *Glyphalina*, *Pupoides*) had D/L Asp values between 0.060 and 0.170, indicating that these shells were introduced into the assemblage after its deposition. The small variance in D/L Asp for succineid shells and the close agreement of multiple radiocarbon shell ages suggests time averaging within individual stratigraphic horizons was on the order of 100 years. Principal components analysis (PCA) of the AAR data showed that the D/L ratios of rapidly-racemizing amino acids (serine, aspartic acid) had strong, positive loadings on the first principle component (PC1), while the concentration of L-Ser had a strong, negative loading. PC1 accounted for 40% and 38% of the variance within the Big Platte and Kulas Quarry data respectively. This component is interpreted to represent a contamination gradient with high L-Serine loading negatively, and a D/L value gradient where higher D/L values load positively. PC2 correlated positively with Depth (distance below surface) and [Sum] (total amino acid concentration; pM/mg shell), whereas high D/L values of slower racemizing amino acids (glutamic acid, alanine) loaded negatively. PC2 accounted for 18% and 24% of the total variation within the data from Big Platte and Kulas Quarry respectively. The negative correlation between depth and D/L Glu and D/L Ala indicates that either L-Ala and L-Glu are preferentially removed (by leaching free amino acids) or D-Ala and D-Glu are introduced at the surface. D/L Asp – an indicator of age – did not correlate, or showed a slight negative correlation with Depth. Surface heating may partially explain stratigraphic aberrations in D/L Asp values. The anomaly in Glu and Ala may be a result of surface contamination from bacteria, as the peptidoglycan in the cell walls of many bacteria is enriched in D-Ala and D-Glu. This has not previously been observed in terrestrial gastropod AAR studies, but has significant implications for future gastropod-based amino acid geochronologic studies – especially where D/L Glu is used as an independent or longer interval (e.g. beyond radiocarbon utility) estimate. Data screening should include an analysis of excessive D-Ala, or bleaching gastropod shells to focus analyses upon intra-crystalline proteins.

### 3.1 INTRODUCTION

The age structure of a fossiliferous deposit is of fundamental importance to its paleoecologic interpretation. The scale of time represented by a deposit – both in terms of the accrued time to assemble the sediment and fossils as well as the time differential between individual shells – controls the types of questions that can be addressed (e.g. Kowaleski et al., 1998). Virtually all fossil accumulations are time-averaged to some extent; individual shells within a deposit may differ in age (i.e. time since death) by tens to tens of thousands of years or more (e.g. Kidwell and Flessa, 1995). Considerable attention has been paid to the age structures of marine shelly deposits (see Carroll et al., 2003 and references therein) and to a lesser extent lacustrine (e.g. Cohen, 1989) or terrestrial deposits (e.g. Goodfriend, 1989; Yanes et al., 2007).

Amino acid racemization (AAR) analyses have become an increasingly important tool for assessing the temporal fidelity of shelly deposits. This technique has several advantages over radiocarbon analyses; the process is quick, relatively inexpensive, and can be carried out on samples as small as a single foraminifer test or ostracod valve (e.g. Kaufman, 2000; Kaufman, 2006). Amino acid geochronology is a relative-dating method or, when coupled with numerical methods like radiocarbon, a calibrated-dating tool. It can therefore be used to address important paleoecological questions such as time averaging within fossil deposits (e.g. Carroll et al., 2003), paleotemperature estimates (e.g. Kaufman, 2003), and stratigraphic correlation (e.g. Miller and Hare, 1980; Miller et al., 1987).

In addition, many late Pleistocene terrestrial fossil assemblages include species whose modern ranges do not overlap (i.e. non-analog faunas; Graham and Meade, 1987).

The question of whether these non-analog faunas result from individual responses to past climate change by specific taxa, or post-mortem mixing of fossil remains is of fundamental importance (e.g. Stafford et al., 1997). The combined problems of time-averaging and non-analog faunas can lead to erroneous paleoclimatic interpretations. Previous studies have often focused on primary loess deposits, because it is assumed that their degree of temporal and spatial mixing has been negligible (e.g. La Rocque, 1970; Hubricht, 1985). Combined use of AAR and radiocarbon can improve our understanding of the temporal fidelity of fossil assemblages.

Amino acid analyses result in a large amount of raw data with many intercorrelated variables; reduction of the data is necessary to identify the most important influences. Sources of non-temporal variation within AAR data have the potential to strongly affect age-related inferences, but the underlying mechanisms and sources of error are not well understood (e.g. Kosnik and Kaufman, 2008). Modern contamination and diagenetic effects such as leaching of free amino acids are both major concerns with amino acid geochronology. Methods for identifying anomalous results have largely focused on univariate and bivariate statistical analyses (e.g. Kaufman, 2000; Laabs and Kaufman, 2003; Kaufman, 2006; Kosnik and Kaufman, 2008). However, removing anomalous or poorly fitted data increases the risk of rejecting material that may actually represent a fraction of the age-distribution of shells from a fossil deposit.

Late Pleistocene gastropod fossils from the Driftless Area of western Wisconsin represent an abundant, but underutilized, fossil proxy for paleoenvironmental interpretation. These are among the most northern late Pleistocene fossil assemblages in the Midwest (Kuchta et al., 2007b) and they have the potential to characterize local full-

glacial, ca. 24,000 - 18,000 cal. yr BP, conditions near the ice margin in Wisconsin (all dates are given in calibrated calendar years before present unless noted). However, the temporal resolution and fidelity of individual fossil horizons must be addressed before any detailed ecological inferences can be made. This study represents a new application of multivariate statistics (PCA) to study variation within terrestrial gastropod AAR data, and the first AAR study of fossil gastropods from Wisconsin.

The goal of this paper is to use amino acid racemization (AAR) techniques on shells from two radiocarbon-dated fossil localities in order to: 1) determine the relative age relationships of several non-analog species that co-occur within these fossil deposits, 2) describe the amount of time averaging in shells from a single taxon, and 3) identify factors that may affect the quality of the geochronologic signal obtained from AAR analysis (e.g. diagenesis, contamination, etc.) using uni- and multi-variate statistical analyses.

### **3.2 GEOLOGIC BACKGROUND**

This study focuses on two sites in the Driftless Area of western Wisconsin: Big Platte and Kulas Quarry (Figure 3.1). Big Platte is a south-facing colluvial exposure in southwestern Grant County. Kulas Quarry is a large exposure of alluvium on the north side of the Latch Valley in Trempealeau County. These sites were discovered during surveys of fossiliferous outcrops throughout the region (see Chapter 2 of this thesis for a more detailed description). Late Pleistocene sediments throughout western Wisconsin commonly include terrestrial gastropods, which have heretofore gone unstudied. These sites have a similar species composition to other late Pleistocene biotic sites, such as



Elkader and Conklin Quarry in Iowa: all are dominated by gastropod species with modern Cordilleran-Boreal range distributions.

Thick colluvium mantles many of the hillslopes within the Driftless Area, and consists primarily of reworked loess and large clasts of local bedrock. These colluvial sediments grade laterally into alluvial sediments covering the valley floor (Knox, 1989; Mason, 1995). Several researchers have speculated that Driftless Area colluvial deposits resulted from late Pleistocene periglacial activity (ca. 25,000 to 16,000 cal. yr BP), and that these sediments were relatively stable during the Holocene (e.g. Knox, 1989; Mason and Knox, 1997). Alternatively, Black (1969) proposed that increased Holocene precipitation induced colluvial activity.

Late Wisconsinan alluvial sedimentation is characterized by valley aggradation in braided streams with a high sediment bedload (Knox, 1996). In river valleys not directly affected by glacial meltwater, much of this sediment consists of weathered bedrock and reworked silt and clay (Mason, 1994). This aggradational phase began by at least 25,000 cal. yr BP and continued until approximately 16,000 cal. yr BP (Flock, 1983; Knox, 1996). Alluvial deposits consist primarily of either vertically aggrading laminated silts and planar-bedded sands, or laterally accreting trough cross-bedded sands and gravels.

### **3.3 METHODS**

#### *3.3.1 Sample collection and processing.*

Samples for AAR and faunal analysis were collected from Big Platte and Kulas Quarry at multiple stratigraphic horizons (Figure 3.2A, B). To minimize the effect of elevated surface temperatures on the rate of racemization, it is recommended that samples

come from at least 1 m depth (e.g. Goodfriend, 1992). At Big Platte, sample depths were constrained by the narrow distribution of the fossiliferous material and the need for stratigraphic control of each sampling horizon. The distribution of shells within the Big Platte exposure was limited: most shells were retrieved from the upper half of the exposure, whereas only a few shells were retrieved from the base. At Big Platte, a total of eight separate samples were collected at least 30 cm back from the scarp surface. Additional AAR samples were collected with a 60 cm soil auger attached to a cordless drill to retrieve material from further back without disturbing a barbed-wire fence post near the top of the exposure (Figure 3.3A). Based on the length of recently exposed roots and un-vegetated slump blocks below the scarp surface, approximately 50 cm of material had been removed due to mass wasting, likely within the past year. Thus, the minimum depth below the surface prior to collection was approximately 80-100 cm.

The original Kulas Quarry exposure was created when the landowner expanded a borrow pit in the spring of 2006. Based on the geometry of the cut and length of exposed tree roots, approximately 1-2 m of material had recently been removed prior to sample collection. I sampled multiple discrete fossiliferous beds along the exposure face (Figure 3.3B). To facilitate bulk collection of deeper material, the lowest two meters at Kulas Quarry were excavated with a bucket loader by the landowner (Figure 3.3C).

Samples were wet-sieved (smallest mesh = 0.425 mm) and allowed to air dry. Individual shells were picked from the matrix using flexible steel forceps to avoid contamination from modern amino acids (in fingerprints, saliva, etc.). Shells were identified to species (or subspecies) using Pilsbry (1948), Burch (1962), Barthel and Nekola (2000), and reference collections from the University of Iowa Museum of Natural

History. Succineid gastropods cannot be assigned to species without soft-tissue dissection (e.g. Pilsbry, 1948). Shells in my collections were assigned to either “*Succinea* cf. *gelida*” or “*Catinella* cf. *gelida*” based on the size and aspect ratio of the shell aperture; “*Succinea*” shells are generally taller than 1 cm and have an apertural Height:Width ratio greater than 2.0, while “*Catinella*” are much smaller (rarely > 0.5 cm) with an aperture H:W of less than 2.0 (Figure 3.4). Identifications were verified by Jeffery Nekola of the University of New Mexico. Specimens are catalogued and stored at the University of Wisconsin Geology Museum under the catalog number UW1987.

Gastropod taxa found within Big Platte sediments include taxa with Cordilleran-Boreal and Eastern Deciduous Forest ranges (*sensu* Wells and Stewart, 1987; Table 3.1; Figure 3.5A, 3.5B). In general, shells of the latter group were more transparent and less worn compared to the Boreal and Cordilleran taxa (Figure 3.4, 3.6). Succineids were chosen for the bulk of the AAR analyses because of their abundance and quality of preservation at both sites. Additional taxa were chosen for analysis because they either 1) represented the most abundant species at Big Platte, or 2) had shells that were much more “fresh” in appearance and whose ranges were very different from the majority of the species recovered (e.g. Cordilleran-Boreal vs. Eastern Deciduous Forest).

To minimize the effect of intrashell variability (e.g. Carroll, 2003), only the body whorls of *Discus* shells were analyzed; AAR results from other taxa represent whole shell analyses. Some samples of *Succinea* had surface discoloration. These shells were broken and only fragments clear of these black spots were analyzed.

Shells of Eastern Deciduous Forest species were in general much better preserved than those of Cordilleran-Boreal species (Table 3.1; Figure 3.4). Live terrestrial

gastropods often have a glossy and transparent or translucent shell, which becomes increasingly opaque and white with age (M. Kuchta, personal obs., 2007). To test the hypothesis that shell condition reflects age, the shells analyzed for amino acid racemization were graded on a qualitative scale from 1 to 5 based on their condition. This scale ranked the appearance of individual shells where 1 = fully transparent/translucent shell with glossy surface, 2 = partially opaque shell with minor surface wear, 3 = fully opaque shells with little or no surface wear, 4 = fully opaque shell material with dull surface texture, 5 = opaque and dull shell material with significant surface wear (Figure 3.6). These shell condition scores were then compared to the D/L ratios of aspartic and glutamic acids to determine the relationship between relative shell age and appearance. If shells that look younger are significantly different in age, there is justification to eliminate them from subsequent paleoecological reconstruction, and future studies can consider these taxa anomalous when found within fossil deposits.

### *3.3.2 AAR Concept*

Fossil gastropods are well suited for AAR analysis (e.g. Oches and McCoy, 2001). Gastropods synthesize amino acids (such as Aspartic acid) in their L-form (levorotary) to make the proteinaceous matrix that supports their calcareous shells. At death these L-amino acids undergo a reversible inversion (racemization) to their chiral D-form (dextrorotary). This racemization reaches equilibrium when the ratio of D- to L-forms (D/L) of an amino acid equals 1.0. The rate of racemization is a function of temperature and time: D/L ratios will increase over time to the equilibrium point, and will do so more rapidly as ambient temperature increases (McCoy, 1987; Goodfriend, 1992).

Because two separate shells from within the same deposit have shared a similar post-depositional temperature history, the difference in their D/L values can be used to assess the relative age differences between them (e.g. McCoy, 1987; Yanes et al., 2007).

Different molluscan taxa may exhibit different rates of racemization; therefore, taxonomically restricted samples are preferred in order to reduce variation in the measured D/L ratios due to this “vital effect” (Oches et al., 1996; Roof, 1997).

Analyses were carried out at the Amino Acid Geochronology Lab at Northern Arizona University using Reverse-Phase, High-Performance Liquid Chromatography (HPLC) to measure the D/L ratios of several amino acids, including aspartic acid (Asp), glutamic acid (Glu), serine (Ser), and alanine (Ala). Asp and Glu likely include a small amount of asparagines and glutamine, respectively, as these can be converted to Asp and Glu during laboratory hydrolysis. Amino acid compositions reported here reflect the total hydrolysable amino acids (THAA) within the shell, which includes both inter- and intra-crystalline proteins. For detailed methods, see Kaufman and Manley (1988) and updates by Kaufman (2000, 2006).

I focused on Asp and Glu for geochronology because they are among the most clearly resolved with HPLC. Asp racemizes at a much faster rate than does Glu; it is least an order of magnitude faster than the commonly used alloisoleucine/isoleucene (A/I). Glu racemizes at a rate comparable to A/I, and provides a quasi-independent estimation of sample age (Kaufman, 2000; Hearty and Kaufman, 2009). The concentration of the labile amino acid Ser, when compared to concentrations of more stable amino acids, is often used as an indicator of modern contamination (Kaufman, 2000; Kosnik et al., 2008). The general expectation is that D/L values for Asp and Glu will increase over time

(~stratigraphic depth) and/or as increased temperatures accelerate racemization. At mid-latitudes, the effective age range for AAR techniques is typically 2 ma. A description of each variable presented in this study is presented in Table 3.2.

Variation in the diagenetic history of samples can influence measured D/L values. Leaching of free amino acids from the shell, usually enriched in D-amino acids, will yield younger-than-expected D/L ratios (e.g. Roof, 1997). Contamination by modern amino acids (often enriched in L-amino acids, especially L-Ser) will also yield lower D/L values (e.g. Kosnik and Kaufman, 2008). While contamination is generally thought to produce younger-than-expected D/L values, the peptidoglycan within bacterial cell walls is enriched in D-Ala and D-Glu, which may produce an excess of D-amino acids as a result of bacterial growth. Anomalies in the D-amino acid fractions of both Ala and Glu may point to bacterial contamination of the intra-shell amino acids (e.g. Blackwell et al., 2000; Nyberg et al., 2001).

### 3.3.3 Radiocarbon

I obtained radiocarbon dates from succineid gastropod shells. Succineid gastropods are abundant in many late Pleistocene deposits, and are often the only organic material available for radiocarbon dating (e.g. Mason and Knox, 1997; Pigati et al., 2004). There are two primary sources of error in radiocarbon dates obtained from gastropod shells. The first is recrystallization of aragonite to calcite, which can yield younger-than-actual ages. This error can generally be avoided by using shells without visibly recrystallized, “chalky” shell material and by pre-etching the sample in acid before analysis (Goodfriend and Stipp, 1983; Goodfriend and Hood, 1983). The second

problem is harder to detect and occurs when the snail ingests  $^{14}\text{C}$ -depleted carbonate, which can yield anomalously old radiocarbon ages (Goodfriend and Hood, 1983; Goodfriend and Stipp, 1983, Pigati et al., 2004). Succineid gastropods do not appear to ingest old carbonates, even when in a  $^{14}\text{C}$ -depleted carbonate environment. Other gastropods, however, can show significant variation in radiocarbon age because they often ingest these depleted carbonates (e.g. *Vallonia*; Pigati et al., 2004; Rech et al, in prep).

Radiocarbon ages were calibrated to calendar years using the “CalPal-2007<sup>online</sup>” software (Danzeglocke et al., 2007). Additional statistical analyses of radiocarbon results were performed using the Calib 5.1beta program (Stuiver and Reimer, 1993).

### 3.3.4 Data Screening

Non-temporal sources of variation (e.g. contamination or leaching) can have a profound effect on AAR data. Understanding the source of this variation can identify outliers that are truly aberrant, as opposed to older, reworked shells. Identification of AAR outliers is carried out empirically, but no universal standard for recognizing and rejecting outliers exists. A set of screening criteria for one taxon may not be applicable to others. Kaufman (2003) rejected ostracod AAR data when L-Ser/L-Glu ratios exceeded 1.0, whereas Kaufman (2006) rejected foraminiferal AAR data when L-Ser/L-Asp ratios exceeded 0.8 (> 1.5 in degraded samples). Kosnik and Kaufman (2008) compare transformed marine mollusk AAR data to linear models and flag residuals greater than a specified cutoff value.

I followed the suggestions of Kaufman (2000), Kaufman (2006), and Kosnik et al. (2008) to systematically identify outliers in *Succinea*, *Catinella*, and *Helicodiscus* (see Appendix B for further discussion). The remaining taxa consisted of too few individuals to provide reliable outlier estimates. The outlier screens presented here are a modification of those described in the literature (e.g. Kaufman, 2006; Kosnik and Kaufman, 2008) and are based on empirical analysis of the Big Platte and Kulas Quarry data sets. To reduce the influence of screening on the inferred age-population of the shells, I only flagged samples whose residuals were more than three standard deviations outside the mean for a normal distribution. Samples that were flagged by more than one screening test were rejected.

Tests for outliers included the following: 1) the covariance of L-Ser/(L+D Asp) versus D/L Glu. Values of the labile L-Ser should be small; samples with abnormally high L-Ser may indicate modern contamination (e.g. Kaufman, 2000). 2) Covariance of L-Ser/(L+D Glu) with D/L Asp is a quasi-independent test compared to 1 (*sensu* Kosnik and Kaufman, 2008). 3) The concentration of [Asp] and [Glu] should covary as a function of time. Departures from this relationship may indicate aberrant behavior. Total concentration of amino acids ([Sum]) was calculated as the sum of the peak D+L areas within each sample, calibrated to an internal spike of the non-protein amino acid L-*h*Arg (Kaufman, 2000). 4) Finally, D/L Asp and D/L Glu should both increase over time (D/L Asp at a faster rate) and samples that do not display this well-documented covariance may indicate an alternate diagenetic pathway (e.g. Kaufman, 2003). 5) In addition to univariate tests, I used the “Outlier Analysis” option in PC-ORD 5.0 (McCune and Mefford, 2006) to analyze the entire data matrix for outliers within rows (samples). This



method creates a frequency distribution for the calculated average distances between all entities in the matrix and flags multivariate outliers from this distribution at user-defined cutoffs. I transformed the data matrix by subtracting the mean from each variable and dividing by its standard deviation. This transformed matrix represents the total variation within each column. The distances between individual samples were measured using the Euclidean distance measure. I flagged samples whose average distance was more than three standard deviations above the mean average distance for all samples.

### *3.3.5 Statistical analyses of succineid age-structure*

Descriptive statistics and tests were performed in Minitab and PAST (Hammer et al., 2001). The significance of pair-wise ANOVA results was corrected for multiple comparisons using the conservative Bonferonni correction of  $\alpha=0.05/n$  (where  $n$ =total number of within-test comparisons). To test for time-averaging using D/L Asp values as an indication of age, I compared the measured coefficient of variance (C.V. = standard deviation/mean\*100%) for samples of succineid shells at Big Platte and Kulas Quarry to an expected range due to laboratory precision and inter-shell variation. Laboratory precision of D/L Asp measurements is typically  $\leq 5\%$  (Kaufman, 2000). The inter-shell variability in D/L values is unknown for “live-collected,” congeneric shells.

Theoretically, the initial D/L value of live-collected shells should be zero, but a small amount of laboratory-induced racemization occurs during sample hydrolysis (Kaufman, 2000). Furthermore, there are few measurements of amino acids in shells known to have coexisted because remnant soft tissue, or chemical removal of this soft tissue, can significantly alter the D/L ratios of the shell. Hearty and Kaufman (2009) reported D/L

Asp values in shells from museum collections of the terrestrial gastropod *Cerion* from Jamaica that varied between 10 and 25%. These museum collections were acquired over several centuries; the snails analyzed were not alive at the same time. Walther (2004) reported D/L Asp values from three live-collected *Succinea* shells that varied by 18.5%. Terrestrial gastropod fossils in eolian sediments typically have within-horizon C.V.s for D/L Asp values between 10 and 15% (Walther, 2000; Oches et al., 2005; Ortiz et al., 2006). Previous authors have reported between 10% and 20% variation in D/L Asp values from assemblages considered representative of a “single-age” population (e.g. Murray-Wallace, 2000; Yanes et al., 2007). However, because previous studies examined shells not known to exist at exactly the same time and due to the problems associated with accurately measuring D/L Asp values from live shells, I conservatively estimate a truly live-collected population of shells should exhibit 5-10% variation in their measured D/L Asp values.

Principal components analysis (PCA) is an eigenvector-based method of data reduction. The goal of PCA is to reduce a large, multivariate dataset (such as that produced by AAR analysis) to a small number of synthetic variables (eigenvalues) that represent the principal components of the variation within the entire data (see also McCune and Grace, 2002). Previous applications of PCA to amino acid data include characterizing the degradation of organic material in marine sediments (Dauwe and Middleburg, 1998), estimating the influence of taphonomic factors such as shell breakage on the amino acid concentration in brachiopods (Carroll et al., 2003), and determining the amount of variance represented by the D/L values of various amino acids (Ortiz et al., 2006).

PCA is ideally suited to data with approximate linear relationships among variables. Many AAR variables, such as D/L Asp approximate a linear relationship with time over relatively narrow ranges (e.g. D/L Asp values between 0.300 and 0.400; Kaufman, 2000). Although PCA does not require independent variables, it does assume multivariate normality of the data, although this requirement is more relaxed for descriptive purposes (McCune and Grace, 2002). McCune and Grace (2002) suggest that when  $|\text{skew}| < 1$ , PCA performs quite well. However, because PCA seeks the strongest linear correlation among variables, it is highly sensitive to outliers. Therefore, PCA was run after data screening. It is possible to use this technique to identify outliers within the AAR dataset, although this method was not explored in detail for this study.

I used a correlation matrix for the PCA routine, which subtracts the mean from the actual value within each column and divides this by the standard deviation. The reduced data set displays the eigenvalues, or principal component (PC), responsible for the majority of the variation. The first PC represents the greatest variance within the dataset. The second PC accounts for the majority of the remaining variance, and so on. Because each PC is orthogonal to the rest, they are not correlated to one another. Only the first three principal components were calculated, and to determine which were important, I compared the eigenvalues of each PC to the value expected from a random “Broken-Stick” model (e.g. Jolliffe, 2002). If the calculated eigenvalue was greater than the random expectation, the PC was considered significant. *P*-values for each eigenvalue were calculated by the formula suggested by Peres-Neto (2005):

$$p=(n+1)/(N+1)$$

where  $n$  is the number of randomizations with an eigenvalue greater than observed, and  $N$  is the total number of randomizations ( $N=999$ ).

The eigenvalues calculated by PCA can be shown graphically on an ordination diagram where the distance between individual samples (points) approximates their distance in multidimensional space (e.g. McCune and Grace, 2002). Samples that are similar to each other will plot closer together. Samples with values close to the average for all variables will plot near the origin, while outliers will plot much further away (Legendre and Legendre, 1998). The correlation between variables, represented by each eigenvector, is calculated in the cross-product matrix produced during construction of the PCA. Eigenvectors can be plotted on the ordination in a biplot, providing a visual representation of the relative strength of the loading and correlation of the variable to the ordination axes (Legendre and Legendre, 1998). I created a distance-based biplot in PC-ORD 5.0, which scales the eigenvector to its unit length. The length of the vector on the biplot represents its relative loading on a particular component (eigenvalue) and its direction represents its correlation to the eigenvalues (e.g. Legendre and Legendre, 1998; McCune and Grace, 2002). The angles between individual eigenvectors, however, are meaningless, because the ordination is “flattened” into just two dimensions (correlations between vectors are calculated in the cross-product matrix). An object (=sample unit) projected at a right angle to the vector approximates the object’s position along that vector.

### 3.4 RESULTS AND DISCUSSION

Results are presented in the following sequence: 1) first, a summary of the data with results of outlier detection and the samples rejected based on this analysis. Rejected samples are excluded from subsequent analyses. 2) Amino acid differences between taxa based on their range (Cordilleran-Boreal vs. Eastern Deciduous Forest) and shell condition. 3) Relative time averaging and age structure patterns within succineid shells at Big Platte and Kulas Quarry based on radiocarbon and D/L ratios. 4) PCA of Big Platte and Kulas Quarry succineids using the raw AAR data, supplemented by additional univariate analyses of the identified trends.

#### 3.4.1 Data Summary

A total of 236 shells were analyzed for AAR (Appendix A). The shells came from 10 bulk sediment samples at Kulas Quarry (all *Catinella* cf. *gelida*.; n=57), and 179 shells from 8 bulk sediment samples at Big Platte: *Succinea* cf. *bakeri* (n=131), *Helicodiscus parallelus* (n=11), *Discus* sp. (n=7), *Vertigo modesta modesta* (n=6), *Columella columella alticola* (n=6), *Vallonia gracilicosta* (n=5), *Hawaiiia minuscula* (n=5), *Pupilla muscorum* (n=4), *Euconulus fulvus* (n=2), *Pupoides albilabris* (n=1), and *Glyphalinia indentata* (n=1). An AAR “sample” consisted of a single shell from one of these species, identified by a UAL lab number (Appendix A).

Several of these taxa have modern ranges that do not overlap (Figure 3.5A, 3.5B). For example, *Columella columella alticola* is associated with alpine tundra habitats with a Cordilleran-Boreal distribution centered over the Rocky Mountains, whereas *Helicodiscus parallelus* is generally associated with Eastern Deciduous Forests

(Hubricht, 1985). The Cordilleran-Boreal taxa are typically much more abundant compared to those from the Eastern Deciduous Forest (Table 3.1). *Helicodiscus parallelus*, however, is often more abundant in samples than the Cordilleran-Boreal species *Vertigo modesta parietalis* and deciduous forest species that prefer colder climates (i.e. *Euconulus fulvus*, *Disscus whitneyi*; Table 3.1). It is possible that these Eastern Deciduous Forest taxa were introduced after the Cordilleran-Boreal shells were deposited, but, in many cases, the occurrence of a few rare species provides greater insight into the environmental conditions than do the abundant ones (Miller and Bajc, 1987). Therefore, before any environmental reconstruction can be done, separating younger shells from older ones based on D/L AA data is vital.

Data screening of *Succinea*, *Catinella*, and *Helicodiscus* flagged a total of 18 outliers in at least one test. Only seven shells (4 *Succinea*, 2 *Catinella*, 1 *Helicodiscus*), about 3.5% of all analyzed, were flagged in two or more tests and rejected (Table 3.3; Figure 3.7). Three shells (UAL#s 6573J, 6846E, and 6566A) were flagged in a majority of tests, while the others were flagged by one or two tests. Samples that were flagged by one test often did not appear as unusual in another. For example, L-Ser/(D+L Asp) flagged five samples that were not flagged in the L-Ser/(D+L Glu) test. The multivariate distance test was the least conservative, flagging four samples (all of which were rejected), while the covariance of Asp to Glu was more conservative, and identified nine samples as outliers. Setting the cutoff for multivariate distance at two standard deviations resulted in flagging an additional four samples, one of which (UAL# 6849D) was flagged in only one other test and would have been rejected based on this lowered cutoff value (see Appendix B).

### 3.4.2 Amino acid differences between taxa

#### 3.4.2.1 D/L differences by taxon range

The four amino acid D/L ratios measured for each taxon are summarized in Table 3.4, and Figure 3.7, 3.8A). In general, species whose range is currently in the Cordilleran-Boreal regions had significantly higher D/L values than those of Eastern Deciduous Forest species (one-way ANOVA, D/L Asp  $p < 0.001$ ; Table 3.5A). The Cordilleran-Boreal taxa had D/L Asp ratios above 0.250, whereas Eastern Deciduous Forest species had D/L Asp ratios below 0.200 (Figure 3.7, 3.8A). The D/L ratios for the other three amino acids were also lower for Eastern species, and the differences in slow racemizing amino acids (Glu and Ala) were less than differences between fast racemizing amino acids (Asp and Ser; Figure 3.8A). Pairwise comparisons between taxa showed that D/L values for taxa from within a particular province (either Cordilleran-Boreal or Eastern Deciduous Forest) were similar to each other, but significantly different from those of the other province (Table 3.5A, 3.5B). This pattern was most pronounced in the rapidly racemizing amino acids (Asp and Ser). In addition, although there were smaller differences in the absolute values, slowly racemizing amino acids (Glu and Ala) showed the greatest statistical differences between Cordilleran-Boreal taxa. Eastern Deciduous Forest species were not significantly different from each other for any D/L value (Figure 3.8A, Table 3.5A, 3.5B).

#### 3.4.2.2 D/L differences by shell condition

The shells of Eastern Deciduous Forest taxa were generally “fresher” in appearance compared to the Cordilleran-Boreal taxa. These condition scores correlated strongly with D/L ratios; slowly racemizing amino acids displayed stronger and more

significant correlations than did rapidly racemizing amino acids (Table 3.4). Shells with lower condition scores had smaller D/L values compared to shells with high condition scores (Figure 3.8B). D/L values were significantly different between the best-preserved shells (shell condition = 1 or 2) and more weathered shells (shell condition = 3 or 4) (Table 3.6A, 3.6B).

These results show that the well-preserved shells of Eastern Deciduous Forest taxa have significantly lower D/L values than do the lower-quality shells of Cordilleran-Boreal taxa. This suggests that some of the Eastern Deciduous Forest species (*Helicodiscus*, *Glyphalinia*, *Hawaiiia*, and *Pupoides*) were introduced much later, whereas deciduous forest species *Discus whitneyi* and *Euconulus fulvus* were contemporaneous with the Cordilleran-Boreal species. The colluvium was likely deposited during the late Pleistocene as a result of permafrost-induced solifluction (Mason and Knox, 1997), which would account for the abundance of Cordilleran-Boreal taxa with relatively high D/L values. Incorporation of the younger shells could have occurred during the Holocene, when these species adjusted their ranges as a response to climate changes (e.g. Miller and Bajc, 1987). *Glyphalinia*, *Hawaiiia*, and *Helicodiscus* have been reported burrowing into the soil several cm (Pilsbry, 1948; Sparks, 1964). Motter (1898) observed live *Helicodiscus parallelus* and *Hawaiiia miniscula* on exhumed human cadavers. The presence of live gastropods within these graves, all more than 1 m below the surface, indicates an exceptional burrowing capacity for these species. Future paleoecological interpretations of terrestrial gastropod assemblages will have to account for the possibility of introduced species with significantly different climatic preferences. The obvious difference in shell preservation, however, can provide an important first-order



estimate of specimen age. These results contrast with studies from marine shelly assemblages, where taphonomic condition did not correspond well to actual age (e.g. Carroll et al., 2003).

### *3.4.3 Time averaging estimation of succineid shell assemblages*

#### *3.4.3.1 Radiocarbon results*

A total of nine radiocarbon dates were obtained from succineid shells for this study (Table 3.7). Three succineid shells from Big Platte yielded ages between  $18,964 \pm 228$  and  $19,075 \pm 215$  cal yr. BP. Two separate stratigraphic intervals were examined at Kulas Quarry. Samples from KQ05 (depth = 4.5 m) provided two dates at  $20,961 \pm 314$  and  $21,673 \pm 448$  cal yr BP, whereas samples from KQ15 (depth = 2.75 m) provided four dates between  $19,929 \pm 295$  and  $20,617 \pm 330$  cal yr BP. In general, radiocarbon results are consistent with stratigraphic position; shells from the same sample horizon yielded radiocarbon dates within a few hundred years or less of one another (Figure 3.2A, B). Reported age dates were significantly different between sites ( $X^2$ ,  $T=667.9$ ,  $df=8$ ,  $p<0.001$ ; radiocarbon statistical tests performed with Calib 5.1 BETA software; Stuiver and Reimer, 1993). Samples from Big Platte were not significantly different from each other ( $X^2$ ,  $T=4.2$ ,  $df=2$ ,  $p=0.069$ ). Dates from Kulas Quarry samples showed a greater range in reported values from within a selected horizon. The two dates from KQ05 were significantly different at  $\alpha=0.05$ , but not at  $\alpha=0.01$  ( $X^2$ ,  $T=4.31$ ,  $df=1$ ,  $p=0.038$ ), while the three dates from KQ15 reported by the Arizona lab were not significantly different ( $X^2$ ,  $T=4.2$ ,  $df=2$ ,  $p=0.12$ ; Table 3.7).

#### *3.4.3.2 D/L Asp variation in succineids*

The mean D/L Asp values from Big Platte were significantly higher than those of Kulas Quarry (two-sample t-test;  $t=2.747$ ,  $p=0.024$ ; Table 3.4, however the variance for the two sites was similar (test of variance;  $F=1.3098$ ,  $df=1$ ,  $p=0.264$ ). D/L Glu, however, was significantly different in both mean and variance ( $F=2.236$ ,  $df=1$ ,  $p<0.001$ ; unequal variance t-test,  $t=14.17$ ,  $p<0.001$ ). Taken at face value, the D/L Asp values suggest that Big Platte is older than Kulas Quarry, and are at odds with the radiocarbon data that show Kulas Quarry is older than Big Platte. Radiocarbon age results for succineids from Big Platte and Kulas Quarry show that the within-horizon age differences between  $^{14}\text{C}$  measurements was relatively small (ca.  $10^2$  years), and that Kulas Quarry is about  $10^3$  years older than Big Platte. However, the D/L Asp ratio is a function of both time *and* temperature. Most samples from Big Platte were obtained within 1 m of the surface, whereas Kulas Quarry samples were obtained from more than 2 m. Therefore, it is possible that the relatively high D/L Asp values at Big Platte resulted from elevated surface temperatures rather than greater elapsed time. Oches et al. (1996) noted similar “reversals” in amino acid racemization rates in shells obtained from loess from the Upper Mississippi Valley. In addition, groundwater-induced leaching of free amino acids (enriched in D-amino acids) would be more prevalent in the permeable sand at Kulas Quarry, yielding lower D/L values compared to the clay-rich silt at Big Platte.

The coefficients of variance in succineid shells for D/L Asp at Big Platte and Kulas Quarry were about 5% (Table 3.4), which can be attributed to analytical uncertainty. Other Cordilleran-Boreal taxa such as *Discus*, *Columella*, and *Vertigo* had similarly low variance in D/L Asp. The Eastern Deciduous Forest taxa (*Helicodiscus* and *Hawaiiia*) typically had more variability in the D/L Asp values. Some of this variability

can be attributed to sample size, but the large variability in D/L Asp values in *Helicodiscus* compared to those of most Cordilleran-Boreal taxa suggests a much larger range in relative age for *Helicodiscus* shells. The introduction of these younger shells likely occurred over a much longer time range compared to deposition of the initial assemblage. Previous authors have cautioned that alluvial deposits may contain assemblages that are inherently more mixed due to long-range transport and sediment reworking (e.g. La Rocque, 1970; Hubricht, 1985). The range in D/L Asp values from this study is generally less than that reported for stratigraphically restricted samples of late Pleistocene succineids from eolian deposits in North America and Europe (e.g. 12.5% in Oches et al., 2002; and 4-8% in Walther, 2004) and helicids from the Canary Islands (e.g. 3-12% in Ortiz et al., 2006). Thus, based on D/L Asp values, the scale of age mixing within Big Platte (colluvium) and Kulas Quarry (alluvium) appears to be similar to that other terrestrial deposits.

It is also interesting to note that the D/L Asp values for Big Platte and Kulas Quarry were approximately normally distributed (Shapiro-Wilk normality,  $p > 0.5$ ) with relatively low skewness and kurtosis (Table 3.8). Yanes et al. (2007) reported a higher proportion of left-skewed, platykurtic (less peaked than normal) age distributions within stratigraphic samples of helicid gastropods in the Canary Islands than expected if their samples were drawn from a right-skewed population. Time-averaging studies from marine deposits often yielded right skewed, leptokurtic (more peaked than normal) age distributions (Flessa et al., 1993; Carroll et al., 2003; Kidwell et al., 2005). These authors attributed the right-skewed age distributions as a result of rapid burial with brief periods of exposure allowing an exponential decay of shelly material along the marine shelf. The

results from this study compare with Yanes et al. (2007) and suggest that terrestrial shelly deposits may be controlled by different factors.

#### 3.4.4 Amino acid trends in PCA

The summary statistics for the AAR results from all succineid shells used in the PCA ordination indicate that many of the variables approximate a normal distribution ( $|\text{skewness}| < 1$ ; Table 3.8). Some values displayed  $|\text{skew}| > 1$ ; variables that are not normally distributed tend to influence the PCA results more strongly than normally-distributed variables (McCune and Grace, 2002). D/L Ala values were positively skewed for both Big Platte and Kulas Quarry, while L-Ser/(D+L Glu) and D/L Glu showed positive skewness for the Kulas Quarry samples. The eigenvalue and eigenvector results of the PCA for both sites are provided in Tables 3.9 and 3.10, respectively, and plotted as ordination diagrams in Figures 3.9 and 3.10. Only the first two principal components (PC) were considered significant, accounting for about 58% of the variance at Big Platte and 62% of the variance at Kulas Quarry (Table 3.9).

At Big Platte, the first principal component (PC1) is defined by D/L Asp (positive loading; +), D/L Glu (+), D/L Ser (+), L-Ser/D+L-Asp (negative loading; -), and L-Ser/D+L-Glu (-). The second principal component (PC2) is defined by Depth (+), [Sum] (+), D/L Asp (+), D/L Glu (-), and D/L Ala (-) (Table 3.10; Figure 3.9). The PCA results from Kulas Quarry exhibit a pattern of loadings similar to that for the Big Platte analysis on the first two PC's. (Table 3.10; Figure 3.10). PC1 for the Kulas Quarry data loaded most strongly with D/L Asp (+), D/L Ser (+), L-Ser/D+L Asp (-) and L-Ser/D+L Glu (-),

whereas PC2 loaded most strongly with Depth (+), [Sum] (+), D/L Glu (-), D/L Ala (-), and L-Ser/D+L Glu (-).

The cross-product matrix for Big Platte (Table 3.11) showed the strongest positive correlations for the total concentration of amino acids, [Sum] with D/L Asp; racemization of most amino acids, D/L values of Asp, Glu and Ser; and indicators of elevated L-Ser content (D+L-Asp and D+L Glu). The strongest negative correlations were observed for Depth with D/L Glu and D+L Glu, indicators of elevated L-Ser (L-Ser/D+L-Asp and L-Ser/D+L Glu) with D/L Ser; and D/L Glu versus D+L-Asp and D/L Ser.

The ordination scores for individual shells from Big Platte and Kulas Quarry show different distributions along the first two principal components. Shells in the Big Platte ordination plot on both principal components equally. Shells that were taken from shallow stratigraphic sediment samples are more widely dispersed and plot lower on the second component than samples from further below the surface (Figure 3.9). The Kulas Quarry ordination scores for shells from different stratigraphic horizons show more overlap along PC2 and more separation between horizons along PC1 (Figure 3.10). All the shells from stratigraphic horizon KQ18 and one shell from KQ17 plot much further away from the origin than most samples, which may indicate contamination (the shell from KQ17 was flagged as a single-test outlier, but not rejected during screening).

For both localities, PC1 may represent a contamination and higher D/L AA value gradient in that samples with high L-Ser content (a sign of modern contamination) plot further to the left of the origin, while samples with higher D/L Asp and D/L Glu or lower L-Ser (therefore higher D/L Ser) plot to the right. D/L Ala loads weakly on PC1 but in the same direction as the D/L values of other amino acids. At Big Platte, D/L Asp shows

a moderate positive loading on PC1, whereas it shows a weak negative loading on PC1 at Kulas Quarry (Table 3.10). PC2 may represent a gradient for depth, total concentration, and D-isomers of Ala and Glu, related to bacterial contamination. Deeper samples with a higher total amino acid content plot above the origin of both ordinations, while shells with higher D/L Ala and D/L Glu values plot lower.

While these variables load on similar components, they are not necessarily correlated with each other (Table 3.11). In other words, variables that contributed to the total variance did so independently; no single source of variation could be identified with the PCA. At Big Platte, shells from deeper stratigraphic samples (Depth) were negatively correlated with D/L Ala and D/L Glu, whereas Kulas Quarry shells displayed a negative correlation of Depth with D/L Ala, but not D/L Glu. Depth did not directly correlate with [Sum] in either ordination. D/L Glu showed a strong negative correlation with [Sum] at Kulas Quarry, but these variables were not correlated with each other at Big Platte. D/L Ala was weakly correlated with [Sum] in both ordinations.

It is interesting to note that variables expected to increase (Depth, D/L Asp, D/L Glu) or decrease ([Sum]) with time often show either no correlation or are opposite to the expected trend (Table 3.11). Alternate diagenetic pathways than time such as contamination appear to be responsible for the observed results. D/L Asp and D/L Glu are positively correlated in both ordinations, but Depth is negatively correlated with D/L Glu in shells from Big Platte. In addition, [Sum] shows a strong positive correlation with D/L Asp. Typically, high D/L values indicate older, more racemic mixtures, but will also increase if these amino acids had experienced higher temperatures. If surface heating was responsible for this pattern, the D/L values for the less stable amino acids Asp and Ser

should show a strong negative correlation with Depth. There is a small positive correlation between D/L Asp and Depth at Big Platte, but no correlation at Kulas Quarry (Table 3.11). Therefore, surface heating cannot account for the alteration of D/L Asp values at Big Platte. However, several stratigraphic samples from Kulas Quarry were retrieved from similar depths below the surface (Figure 3.2B), which may account for the lack of a relationship between Depth and D/L Asp at this location.

A connection between amino acid concentration, [Sum], and D/L Asp or Depth (~relative age) may exist. As the protein matrix within the shell breaks down, the resulting free amino acids (typically enriched in D-amino acids) are often more susceptible to leaching. Excessively leached shells may produce anomalously younger D/L results (e.g. Roof, 1997; Penkman et al., 2008). [Sum] displayed little correlation with most variables, but a strong positive correlation with D/L Asp at Big Platte, and a strong negative correlation with D/L Glu at Kulas Quarry (Table 3.11). Leaching may account for the observed behavior of D/L Glu at Kulas Quarry, but does not appear to correspond to the trends observed at Big Platte.

Summary statistics of both the Big Platte and Kulas Quarry data revealed that D/L Ala and D/L Glu were the most skewed variables. This departure from a normal distribution is probably contributing to the loading on PC2 (Table 3.8; Figure 3.9, 3.10). In addition, several of the outliers flagged during screening but retained for the PCA, lie further out along PC1 or PC2. Several of these outliers have particularly high D-Glu and D-Ala values, perhaps due to bacterial contamination. Previous authors have attributed anomalous D/L values in the diagenesis of recent mammal bones (Blackwell et al., 2000), marine sediment (Keil et al., 2000; Pedersen et al., 2001; Grutters et al., 2002), and

scleractinian corals (Nyberg et al., 2001) to bacterial growth. Child et al. (1993) isolated several strains of soil and fecal bacteria that produced collagenase between 10° and 12°C, suggesting some microorganisms have the potential to alter collagen D/L values.

Furthermore, the peptidoglycan within the cell walls of bacteria is enriched in D-Glu and D-Ala (Friedman, 1999), and can also contain D-Asp and D-Ser (Pedersen et al., 2002).

Contamination (as L-amino acids on PC1, or D-amino acids on PC2) appears to have a strong relationship to the variance of the data. Because they load on different PCs, modern contamination (high L-Ser/(D+L AA)) appears to be independent of where in the section a sample was retrieved (Depth; Figures 3.9, 3.10). However, the negative correlations of Depth with D/L Glu and D/L Ala at Big Platte, and Depth with D/L-Ala at Kulas Quarry suggests shallow stratigraphic samples are more likely to be enriched in D-Glu and D-Ala (Table 3.12). Given the locations of Big Platte and Kulas Quarry near agricultural activity, especially livestock and manure, surficial bacterial contamination is a plausible explanation for much of the observed variation in the D/L values. Kaufman (2000, unpublished data) noted elevated D/L values of Ala and Ser, decreased amino acid concentrations, and visual evidence of microbial attack upon gastropod shells subjected to extensive bacterial activity. Child et al. (1993) noted the presence of bacterial enzymes that could preferentially alter specific amino acids in bone collagen. Therefore, sample collection and processing that attempt to minimize bacterial contamination may not be feasible: bacterial contamination may only be detected with anomalous data.

The Big Platte *Succinea* AAR data reveals that some shells have D-Ala values that do not appear to covary with other peak-measured amino acids (such as L-Ala, as shown in Figure 3.11). Decomposition of Ser to Ala may account for some of the higher



D-Ala values, however, the lack of covariance with any L- or D-amino acid suggests this could be from D-Ala that is added from an external source. A logarithmic transformation of the D/L Ala values would reduce the skewness of this variable, however, transformation of D/L Glu would preclude its chronologic utility.

### 3.5 CONCLUSIONS

#### 3.5.1 Summary

This study demonstrates the potential applications as well as the potential difficulties of applying AAR techniques to fossil gastropods from the study area. A summary of the findings:

1). The gastropod fossils from the Big Platte locality include both Eastern Deciduous Forest and Cordilleran-Boreal taxa, which appear to comprise a non-analog fauna. However, analysis of D/L Asp values from individual shells indicates several Eastern Deciduous Forest taxa (*Helicodiscus*, *Glyphalinia*, *Pupoides*, *Hawaiiia*) are much younger and may have burrowed into the soil, becoming incorporated with the assemblage after deposition. The non-analog component of the Big Platte fauna is partially a result of post-depositional processes, and not attributable to climatic influences.

2). Radiocarbon and D/L Asp results from succineids show minor age differences between shells. Radiocarbon dates on individual shells suggests the degree of age mixing within a stratigraphic horizon may be only a few hundred years; D/L Asp values for succineid shells were well within the range of analytical uncertainty. While younger shells were occasionally introduced after deposition, the shells of Cordilleran-Boreal taxa

show relatively little time averaging. The rare Eastern Deciduous Forest taxa (*Euconulus fulvus*, *Discus whitneyi*) that were identified as late Pleistocene in age are generally widespread and common throughout their range today (Leonard, 1952). This suggests that the late Pleistocene climate may have been similar to those areas where they are rare today; climate reconstructions should not be based on the entire range of these widespread taxa.

3). Principal Component Analysis (PCA) of the amino acid data loaded most strongly on the first component (PC1) with L-Ser (negative) and D/L AA values (positive), perhaps as a result of modern contamination with L-amino acids. The second component (PC2) loaded most strongly with Depth and [Sum] (positive) and D-Ala, D-Glu (negative), which might indicate bacterial decomposition of shell protein and introduction of D-amino acids. Using multivariate statistical techniques, it is possible to observe the net effects of alteration on the entire data set; these anomalies may be overlooked by univariate analysis and screening methods.

Conventional AAR studies measure the total hydrolysable amino acids within gastropod shells, which may be susceptible to contamination (as suggested in this study). Alternatively, intra-crystalline shell proteins appear to behave as a closed system and may be preferable for high-resolution AAR studies (e.g. Penkman et al, 2008) especially from sites at high risk for significant contamination. In addition, data screening can be complex and rejection criteria will vary depending upon the research question of interest. Data that appear “normal” in one variable may be aberrant in another. For example, shells that displayed a relatively normal distribution of D/L Asp values sometimes contained aberrant values for other amino acids (such as D/L Glu or D/L Ala). Whether these

aberrant amino acids affect other values is not known at this time. Data screening for AAR is unique to each situation and a universal set of cutoff points has not been determined (e.g. Kosnik and Kaufman, 2008). Based on these results, additional screening methods to identify aberrant D-Glu and D-Ala values may reveal potentially contaminated samples.

### 3.5.2 Taxonomic AAR trends

The gastropod assemblage recovered at Big Platte contained several non-analog species whose modern ranges include both Cordilleran-Boreal and Eastern Deciduous Forest distributions. Eastern Deciduous Forest species are unique in that they have climate preferences incompatible with the inferred conditions found during the late Pleistocene and their shells appeared considerably newer (Figure 3.8B). The D/L ratios of these shells confirmed that the Eastern Deciduous Forest taxa were considerably younger, having been incorporated into the assemblage after deposition. *Euconulus fulvus* and *Vallonia gracilicosta*, however, are also relatively temperate species. Based on the similarity of the D/L values, these taxa appeared to be contemporaneous with the remaining late Pleistocene gastropod fauna at Big Platte. The presence of these temperate species in the Upper Mississippi Valley at the same time as colder, Cordilleran-Boreal species supports the interpretation by Baker et al. (1986) and Woodman et al. (1996) that conditions were colder, but more equable – with less extremes in summer and winter temperatures – than today.

There were significant differences in the amino acid data of the gastropods from this study. If the influence of microbial activity is relatively small, the variation of amino

acids in succineid shells may be due to taxonomic differences, which would support the conclusions of others (e.g. Oches et al., 1996) that individual genera can yield significantly different D/L values. However, succineids pose a taxonomic problem, due to the morphological similarities of their shells. It is difficult to identify succineids to genus, let alone species, based on shell characters. The large differences observed between *Succinea* and *Catinella* from this study have implications for future paleotemperature gradient studies (e.g. Oches et al., 1996) that compare D/L values in different succineid taxa.

### 3.5.3 Time averaging of succineids

Based on the radiocarbon and AAR results, it appears that individual horizons at Big Platte and Kulas Quarry are not time-averaged on a scale detectable with AAR. In contrast, radiocarbon results do suggest that the age difference between shells *within* a sample horizon is small, perhaps less than 100 years for Big Platte (Table 3.7). The multiple dates from each stratigraphic horizon at Kulas Quarry are within ca. 700 years of each other. Ages between the KQ-15 and KQ-05 horizons at Kulas Quarry indicate these samples are separated by at least 1,000 years, yet the differences in their D/L Asp values are quite small, perhaps as a partial result of surface heating, which could have increased the D/L Asp values at Big Platte and the stratigraphic samples from Kulas Quarry at similar depths. Interestingly, D/L Asp and D/L Glu ratios from Big Platte are higher than those at Kulas Quarry, even though the latter is over 1,000 years older. The significant difference in the mean D/L Asp values may be a result of differential heating, leaching, and/or contamination. However, the variance of D/L Asp values at Kulas Quarry is not

significantly different from the D/L Asp variance at Big Platt and suggests the overall variance in each deposit may represent similar magnitudes of time averaging, or diagenetic alteration.

Previous AAR studies of shelly faunas from marine settings showed significantly right-skewed, leptokurtic distributions of estimated age values, which have been interpreted as a result of time averaging and an exponential loss of older specimens (Flessa et al., 1993; Kowaleski et al., 1998; Carroll et al., 2003; Kidwell et al., 2005). Terrestrial shell assemblages may be subject to different taphonomic mechanisms compared to marine ones; the duration of sediment deposition and possibilities for shell reworking may be reduced (e.g. Yanes et al., 2007), however, the data presented here do not point to any particular taphonomic bias. The range of D/L Asp ratios observed at Big Platte (colluvium) and Kulas Quarry (alluvium) are similar to the ranges reported from loess (e.g. Oches et al., 2002). In addition, the radiocarbon results from this study indicate similar ages between shells. Much concern has been raised regarding the temporal fidelity of gastropod fossils within alluvial deposits due to uncertainties in the reworking and mixing of shells during sediment transport and deposition (e.g. LaRocque, 1970; Hubricht, 1985). These results suggest that alluvial deposition is not an *a priori* reason to ignore the shells contained within these deposits.

#### *3.5.4 Trends from Principal Component Analysis*

The results of this study demonstrate the utility of PCA for analyzing AAR data. Previous studies have mentioned the redundancy and covariance of D/L values for multiple amino acids as a method of error checking and independent chronometers (e.g.

Kaufman, 2003). Ordinations of shells from both Big Platte and Kulas Quarry showed the same general patterns in the loadings on each principal component (Table 3.10; Figures 3.9, 3.10). I interpret PC1 to represent a gradient of L-Ser (negative correlation; modern contamination) and higher D/L AA values (positive). PC2 likely represents a gradient of Depth and [Sum] (positive correlation) and bacterial contamination with D-Glu and D-Ala (negative). This may be a result of bacterial attack on the shells, which would account for higher D-Ala and D-Glu and breaking down shell proteins (lower total AA concentration) near the surface.

While a positive correlation among D/L values is expected as a result of increased racemization with time and diagenesis, several of these results appear to be contradictory. If surface heating was responsible for the higher D/L Asp values at Big Platte, there should be a *negative* correlation between D/L Asp and Depth, since deeper samples would be insulated and therefore less racemic. If the increase of D/L Asp with Depth shown in Figure 3.9 was a result of leaching near the surface (thereby preferentially removing free, D-Asp), D/L values for one or more of the other amino acids (particularly labile Ser) should show a similar trend, and [Sum] would be expected to decrease as these amino acids are removed from samples close to the surface. Finally, D/L ratios of the slow racemizing amino acids Glu and Ala decrease with Depth (Table 3.11; Figures 3.9, 3.10). While leaching of amino acids can account for the increase in total concentration with Depth, this leaching would preferentially remove free amino acids, which are generally enriched in their D- forms. Surface heating may account for the correlation of D/L Asp with Depth at Big Platte given the proximity of these samples to the surface. In contrast, D/L Asp shows almost no correlation with Depth at Kulas Quarry, which may

be partly a function of the increased depth (>2 m) at this site from which stratigraphic samples were taken.

The strong negative correlation between Depth and D/L Glu and D/L Ala suggests a relative decrease in the proportion of their L-amino acids. Because D/L Asp is either positively or un-correlated with Depth and D/L Ser shows no correlation, heating and leaching alone are insufficient to explain this pattern. Near-surface bacterial contamination of Big Platte and Kulas Quarry samples with D-amino acids (particularly D-Ala and D-Glu) would account for this trend. Bacterial enrichment in D-amino acids would be more prevalent near the surface, and it would explain why samples were flagged as outliers in some tests, but not in others. Addition of D-Glu or D-Ala would skew only the results of those tests that look for variation in the relative proportions of specific D-amino acids.

The implications of bacterial contamination are unknown. This pattern has not been previously observed in gastropod shells, although it has been noted in terrestrial mammal bones and marine corals (Blackwell, et al., 2000; Nyberg et al., 2001). Regardless, bacterial alteration of the D/L Glu ratio independently of D/L Asp reduces the utility of these variables as independent tests of age (e.g. Kaufman, 2000). The potential for bacterial contamination to affect future AAR analyses seems high, given the proximity of many fossil localities in the Upper Mississippi Valley to agricultural centers. By comparison, the lack of correlation between L-Serine and Depth suggests that this contamination occurs during or after sample collection (since all samples are collected and processed using the same methods regardless of depth). Reduction of this source of contamination may be as simple as wearing latex gloves during sample collection and

processing. While transformation of the data can reduce the influence of these processes, using D/L Glu as a chronometer will require refined data screening techniques.

The results presented here suggest potential avenues of future work. The lack of correlation between D/L Asp and either radiocarbon or stratigraphic results prevented making a calibrated AAR time/temperature from this data. Given the demonstrated influence of contamination on these results, analysis of intercrystalline proteins may provide more robust results for geochronological estimates (e.g. Penkman et al., 2008). In order to assess the influence of microbial activity, it would be informative (although non-trivial) to culture bacteria from individual shells and examine the shell surface with an SEM to look for microbial traces. Data screening methods should include testing for aberrant values for D-Glu and D-Ala, (e.g. Figure 3.11) which are present in high quantities within bacterial peptidoglycan. Although shell condition has been shown not to be an indicator of age in marine shelf deposits (e.g. Carroll et al., 2003), clear, glossy shells in Quaternary terrestrial sediments may indicate younger shells (e.g. Plug, 1990) have been incorporated into the assemblage.

The non-temporal influences on the AAR data suggest additional screening will be necessary if this method is to be applied to other fossiliferous deposits in Wisconsin. Moscow Fissure (Foley, 1984) contained numerous boreal and deciduous forest vertebrate taxa. A one-kilogram bulk sample of snake vertebrae from this site yielded a full-glacial age for the site (ca. 21,000 cal yr BP). The few gastropods described were all Eastern Deciduous Forest species. AAR analysis of the gastropods from this site may shed light on this fauna. In addition, if shelly material can be retrieved from pre Late



Wisconsin sediments, the methods described here may provide useful to constrain the timing of these earlier events.

### **3.6 ACKNOWLEDGEMENTS**

This research has been made possible through grants from the American Malacological Society, the Geological Society of America, and the Sharon Meinholz Memorial student research and Cline-Dott-Pray funds from the University of Wisconsin-Madison Department of Geology and Geophysics. Darrell Kaufman and Jordan Bright (Northern Arizona Geochronology Laboratory) analyzed the ten-dozen shells I sent – each packed in its own tiny plastic capsule – and provided vital help with interpretation of the results. Jason Rech (Miami, Ohio), Jeff Pigati (Arizona AMS laboratory), and Jeffery Nekola (University of New Mexico) provided their expertise regarding gastropod paleoecology and provided radiocarbon dates for several samples. Richard Slaughter, Matthew Tibbits, and Bridget Diem assisted in the field and laboratory. The Geology departments at both UW-Madison and UMD provided laboratory resources to complete this study. I would especially like to thank the landowners for access to their properties: Richard Kulas (Kulas Quarry) and the Fritz Family (Big Platte). Mr. Kulas also graciously offered his time and equipment to help clear away material covering the lower section of the Kulas Quarry exposure. Finally, Amanda Little reviewed earlier versions of this manuscript.

Table 3.1. Brief description of the distribution and habitat affinity for taxa discussed in text. Big Platte Fauna (shell counts) provided to illustrate relative abundance of individual species. See range maps in Figure 3.5A and 3.5B.

<b>Taxon</b>	<b>Province</b>	<b>Ecology</b>	<b>Big Platte Fauna</b>
<i>Columella columella alticola</i>	C-B	Very cold, moist, willow scrub, high elevations often above 2000m elevation.	357
<i>Pupilla muscorum</i>	C-B	Dry, open arctic, catholic spp.	96
<i>Vertigo modesta modesta</i>	C-B	Willow-birch thickets, cold, moist	561
<i>Discus shimeki</i>	C	Cold, montane forest above 2000m elevation	498
<i>Discus whitneyi</i>	W	Cold, moist to dry, open to forest habitats; warmer habitats than <i>D. shimeki</i> .	4
<i>Vallonia gracilicosta</i>	C-B	Dry, open environments.	28
<i>Euconulus fulvus</i>	C-B (EDF)	Widespread, moist to dry environments, most common in northern regions.	8
<i>Catinella cf. gelida</i>	MW	Common late Pleistocene fossil throughout Midwest, relict in UMW (Frest, 1987).	131
<i>Succinea cf. bakeri</i>	MW	Common in fossil assemblages from Nebraska to Illinois, thought to be extinct.	1848
<i>Helicodiscus parallelus</i>	EDF	Prefers humid woodlands, range extends from Newfoundland west to the plains border.	24
<i>Hawaiiia miniscula</i>	W (EDF)	Widespread from Alaska to Newfoundland and south to Mexico. Typically found in more forested habitats.	13
<i>Pupoides albilabris</i>	EDF	Found under leaf litter in moist woodlands to dry, open grasslands.	4
<i>Glyphalinia indentata</i>	EDF	Common in woodlands, occasionally found in more open areas.	3

Notes: C-B = Cordilleran-Boreal distribution, C = Cordilleran, W = widespread, EDF = Eastern Deciduous Forest, MW = Midwest Biome (Frest and Fay, 1980). Big Platte Fauna obtained from 72.6 kg of sediment,  $N=3575$  shells, note relative paucity of some EDF fauna (e.g. *Glyphalinia*) but not *Helicodiscus*. Shells analyzed for AAR include 55 shells of *Catinella cf. gelida* from Kulas Quarry.

Table 3.2. Description of AAR variables used in this study and their abbreviations.

Variable	Description
<b>D/L Asp</b>	Ratio of D- to L-Aspartic Acid. Racemizes quickly, one of most commonly used aminochronologic measures with HPLC (e.g. Kaufman, 2000).
<b>D/L Glu</b>	Ratio of D- to L-Glutamic Acid. Racemizes more slowly than Asp. Together with Asp are abundant in mollusk shell protein and among most precisely resolved AA's.
<b>D/L Ser</b>	Ratio of D- to L-Serine. Racemizes quickly; very labile with complicated racimization and decomposition kinetics. Excessive L-Ser indicative of modern contamination.
<b>D/L Ala</b>	Ratio of D- to L-Alanine (Ala). A slow racemizer, it is also a byproduct of Ser decomposition (e.g. Collins and Riley, 2000).
<b>L-Ser/(D+L Asp)</b>	Ratio of L-Serine to total Aspartic Acid. High L-Ser values indicate contamination by modern AA's (e.g. Kosnik and Kaufman, 2008).
<b>L-Ser/(D+L Glu)</b>	Ratio of L-Serine to total Glutamic Acid. When plotted against D/L Asp, serves as a quasi-independent test of contamination with L-Ser/(D+L Asp) vs. D/L Glu.
<b>[Asp]</b>	Concentration of Aspartic Acid (pM per Mg shell), calibrated to internal spike of L- <i>h</i> Arg during analysis by HPLC (Kaufman and Manley, 1998).
<b>[Glu]</b>	Concentration of Glutamic Acid, should covary with [Asp] (e.g. Kosnik and Kaufman, 2008).
<b>[Ser]</b>	Concentration of Serine. Very unstable AA, present in shelly material at low concentrations, high [Ser] values often indicate contamination (e.g. Kaufman, 2006).
<b>[Ala]</b>	Concentration of Alanine.
<b>[Sum]</b>	Total concentration of Asp+Glu+Ser+Ala (pM per Mg shell). In general, concentration should decrease with time as organic material degrades and is lost from shell.

Note: L-Ser and "D+L AA" values determined from peak areas measured by HPLC, while concentrations were calibrated to the internal spike of synthetic L-*h*Arg.

Table 3.3. Outliers flagged during screening. Note that samples that flagged in more than one test were rejected.

UAL#	Samp. Loc.	Taxon	Screening Criterion:					#
			D+L Asp	D+L Glu	D/L-Glu, D/L-Asp	[Asp], [Glu]	MV	
<b>6573J</b>	<b>BP-C1a</b>	<b><i>Succinea</i></b>		<b>X</b>	<b>X</b>	<b>X</b>	<b>X</b>	<b>4</b>
6303A	BP-C1a	<i>Succinea</i>				X		1
6303B	BP-C1a	<i>Succinea</i>				X		1
6572A	BP-C1b	<i>Succinea</i>				X		1
6572N	BP-C1b	<i>Succinea</i>	X					1
<b>6572R</b>	<b>BP-C1b</b>	<b><i>Succinea</i></b>	<b>X</b>		<b>X</b>			<b>2</b>
6329E	BP-C1c	<i>Succinea</i>	X					1
<b>6570B</b>	<b>BP-C1d</b>	<b><i>Succinea</i></b>				<b>X</b>	<b>X</b>	<b>2</b>
<b>6330D</b>	<b>BP-C2a</b>	<b><i>Succinea</i></b>	<b>X</b>	<b>X</b>				<b>2</b>
6574C	BP-C2a	<i>Succinea</i>		X				1
6574F	BP-C2a	<i>Succinea</i>				X		1
6331A	BP-C3a	<i>Succinea</i>	X					1
6331C	BP-C3a	<i>Succinea</i>	X					1
<b>6846E</b>	<b>KQ-09</b>	<b><i>Catinella</i></b>	<b>X</b>	<b>X</b>	<b>X</b>	<b>X</b>	<b>X</b>	<b>5</b>
6849D	KQ-15	<i>Catinella</i>				X		1
<b>6850C</b>	<b>KQ-17</b>	<b><i>Catinella</i></b>	<b>X</b>	<b>X</b>				<b>2</b>
6850F	KQ-17	<i>Catinella</i>			X			1
<b>6566A</b>	<b>BP-C1a</b>	<b><i>Helicodiscus</i></b>	<b>X</b>	<b>X</b>	<b>X</b>	<b>X</b>	<b>X</b>	<b>4</b>

Notes: **X** indicates sample was flagged as a 3 $\sigma$  outlier; **D+L Asp** = covariances of L-Ser/(D+L Asp) vs. D/L Glu; **D+L Glu** = covar of L-Ser/(D+L Glu) vs. D/L Asp; **MV** = multivariate euclidean distance; **#** = total number of shells flagged by screening criterion; rejected outliers (7 shells) in boldface type.

Table 3.4. AAR summary data for all taxa. *Catinella* shells are from Kulas Quarry, while the remaining shells are from the Big Platte Fauna.

TAXON	n	D/L Asp			D/L Glu			D/L Ser			D/L Ala			S.C.
		mean	$\pm 1\sigma$	CV	mean	$\pm 1\sigma$	CV	mean	$\pm 1\sigma$	CV	mean	$\pm 1\sigma$	CV	
<i>Succinea</i>	127	0.333	0.019	5.60	0.099	0.007	6.73	0.541	0.055	10.18	0.190	0.034	17.89	3
<i>Catinella</i>	55	0.327	0.016	4.98	0.078	0.010	12.74	0.496	0.060	12.13	0.136	0.015	11.03	3
<i>Discus</i>	7	0.331	0.026	7.92	0.088	0.008	9.16	0.479	0.044	9.19	0.193	0.021	10.88	3.17
<i>Vertigo</i>	6	0.336	0.013	3.82	0.111	0.003	2.64	0.510	0.047	9.29	0.284	0.013	4.58	3
<i>Columella</i>	6	0.296	0.020	6.74	0.121	0.019	15.54	0.437	0.062	14.07	0.282	0.023	8.16	3.17
<i>Vallonia</i>	5	0.283	0.054	19.16	0.074	0.019	25.27	0.365	0.129	35.37	0.141	0.018	12.77	3.6
<i>Pupilla</i>	4	0.333	0.009	2.72	0.124	0.019	15.62	0.507	0.043	8.47	0.330	0.051	15.45	3.5
<i>Euconulus</i>	2	0.322	0.006	1.98	0.109	0.005	4.56	0.520	0.003	0.54	0.221	0.001	0.45	3
<i>Helicodiscus</i>	10	0.141	0.037	26.38	0.046	0.013	28.67	0.168	0.050	29.64	0.069	0.019	27.54	2.1
<i>Hawaii</i>	5	0.111	0.046	41.01	0.046	0.011	23.64	0.128	0.055	42.87	0.061	0.019	31.15	2
<i>Pupoides</i>	1	0.081	NA	NA	0.032	NA	NA	0.118	NA	NA	0.032	NA	NA	1
<i>Glyphalinia</i>	1	0.139	NA	NA	0.040	NA	NA	0.166	NA	NA	0.050	NA	NA	1
Spearman-Rho		0.575			0.712			0.500			0.754			
P-value		0.050			0.009			0.000			0.005			

Notes: n=total number of shells analyzed (whole shell analyzed, except for *Discus*); CV=coefficient of variance = (SD/mean)\*100; S.C. = shell "taphonomic score." Spearman-Rho correlation coefficient calculated by shell condition versus D/L of each amino acid (Wessa.net CITE).

Table 3.5. Pairwise ANOVA results for D/L values by taxon. Comparisons for each amino acid are grouped in the upper right, or lower left.

**A:** Tukey's pairwise comparisons, *p-val* by taxon. D/L Asp (upper right) and D/L Glu (lower left)

	<i>Succinea</i>	<i>Catinella</i>	<i>Discus</i>	<i>Vertigo</i>	<i>Columella</i>	<i>Vallonia</i>	<i>Pupilla</i>	<i>Euconulus</i>	<i>Helicodiscus</i>	<i>Hawaiiia</i>	<i>Pup/Gly</i>
<i>Succinea</i>		1.000	1.000	1.000	0.096	<b>0.011</b>	1.000	0.906	<b>&lt;0.001</b>	<b>&lt;0.001</b>	<b>&lt;0.001</b>
<i>Catinella</i>	<b>0.008</b>		1.000	1.000	0.305	0.057	1.000	0.994	<b>&lt;0.001</b>	<b>&lt;0.001</b>	<b>&lt;0.001</b>
<i>Discus</i>	0.711	0.753		1.000	0.164	<b>0.023</b>	1.000	0.963	<b>&lt;0.001</b>	<b>&lt;0.001</b>	<b>&lt;0.001</b>
<i>Vertigo</i>	0.434	<b>&lt;0.001</b>	<b>0.001</b>		0.060	<b>0.006</b>	1.000	0.832	<b>&lt;0.001</b>	<b>&lt;0.001</b>	<b>&lt;0.001</b>
<i>Columella</i>	<b>0.002</b>	<b>&lt;0.001</b>	<b>&lt;0.001</b>	0.790		1.000	0.118	0.935	<b>&lt;0.001</b>	<b>&lt;0.001</b>	<b>&lt;0.001</b>
<i>Vallonia</i>	<b>0.001</b>	1.000	0.324	<b>&lt;0.001</b>	<b>&lt;0.001</b>		<b>0.015</b>	0.556	<b>&lt;0.001</b>	<b>&lt;0.001</b>	<b>&lt;0.001</b>
<i>Pupilla</i>	<b>&lt;0.001</b>	<b>&lt;0.001</b>	<b>&lt;0.001</b>	0.414	1.000	<b>&lt;0.001</b>		0.932	<b>&lt;0.001</b>	<b>&lt;0.001</b>	<b>&lt;0.001</b>
<i>Euconulus</i>	0.774	<b>&lt;0.001</b>	<b>0.009</b>	1.000	0.456	<b>&lt;0.001</b>	0.153		<b>&lt;0.001</b>	<b>&lt;0.001</b>	<b>&lt;0.001</b>
<i>Helicodiscus</i>	<b>&lt;0.001</b>	<b>&lt;0.001</b>	<b>&lt;0.001</b>	<b>&lt;0.001</b>	<b>&lt;0.001</b>	<b>&lt;0.001</b>	<b>&lt;0.001</b>			0.519	0.456
<i>Hawaiiia</i>	<b>&lt;0.001</b>	<b>&lt;0.001</b>	<b>&lt;0.001</b>	<b>&lt;0.001</b>	<b>&lt;0.001</b>	<b>&lt;0.001</b>	<b>&lt;0.001</b>	<b>&lt;0.001</b>	1.000		1.000
<i>Pup/Gly</i>	<b>&lt;0.001</b>	<b>&lt;0.001</b>	<b>&lt;0.001</b>	<b>&lt;0.001</b>	<b>&lt;0.001</b>	<b>&lt;0.001</b>	<b>&lt;0.001</b>	<b>&lt;0.001</b>	0.793	0.814	

1-Way ANOVA, unequal var: D/L Asp (F=31.4, df=12.07, p<0.001); D/L Glu (F=62.5, df=11.83, p<0.001)

**B:** Tukey's pairwise comparisons, *p-val* by taxon. D/L Ser (upper right) and D/L Ala (lower left)

	<i>Succinea</i>	<i>Catinella</i>	<i>Discus</i>	<i>Vertigo</i>	<i>Columella</i>	<i>Vallonia</i>	<i>Pupilla</i>	<i>Euconulus</i>	<i>Helicodiscus</i>	<i>Hawaiiia</i>	<i>Pup/Gly</i>
<i>Succinea</i>		0.981	0.840	0.999	0.151	<b>&lt;0.001</b>	0.998	1.000	<b>&lt;0.001</b>	<b>&lt;0.001</b>	<b>&lt;0.001</b>
<i>Catinella</i>	0.110		1.000	1.000	0.884	<b>0.017</b>	1.000	1.000	<b>&lt;0.001</b>	<b>&lt;0.001</b>	<b>&lt;0.001</b>
<i>Discus</i>	1.000	0.077		0.999	0.989	0.077	1.000	0.990	<b>&lt;0.001</b>	<b>&lt;0.001</b>	<b>&lt;0.001</b>
<i>Vertigo</i>	<b>&lt;0.001</b>	<b>&lt;0.001</b>	<b>&lt;0.001</b>		0.663	<b>0.004</b>	1.000	1.000	<b>&lt;0.001</b>	<b>&lt;0.001</b>	<b>&lt;0.001</b>
<i>Columella</i>	<b>&lt;0.001</b>	<b>&lt;0.001</b>	<b>&lt;0.001</b>	1.000		0.685	0.730	0.472	<b>&lt;0.001</b>	<b>&lt;0.001</b>	<b>&lt;0.001</b>
<i>Vallonia</i>	0.207	1.000	0.153	<b>&lt;0.001</b>	<b>&lt;0.001</b>		<b>0.006</b>	<b>0.001</b>	<b>&lt;0.001</b>	<b>&lt;0.001</b>	<b>&lt;0.001</b>
<i>Pupilla</i>	<b>&lt;0.001</b>	<b>&lt;0.001</b>	<b>&lt;0.001</b>	0.295	0.240	<b>&lt;0.001</b>		1.000	<b>&lt;0.001</b>	<b>&lt;0.001</b>	<b>&lt;0.001</b>
<i>Euconulus</i>	0.865	<b>&lt;0.001</b>	0.916	<b>0.023</b>	0.033	0.001	<b>&lt;0.001</b>		<b>&lt;0.001</b>	<b>&lt;0.001</b>	<b>&lt;0.001</b>
<i>Helicodiscus</i>	<b>&lt;0.001</b>	<b>0.012</b>	<b>&lt;0.001</b>	<b>&lt;0.001</b>	<b>&lt;0.001</b>	<b>0.004</b>	<b>&lt;0.001</b>	<b>&lt;0.001</b>		0.992	1.000
<i>Hawaiiia</i>	<b>&lt;0.001</b>	<b>0.002</b>	<b>&lt;0.001</b>	<b>&lt;0.001</b>	<b>&lt;0.001</b>	<b>0.001</b>	<b>&lt;0.001</b>	<b>&lt;0.001</b>	1.000		1.000
<i>Pup/Gly</i>	<b>&lt;0.001</b>	<b>&lt;0.001</b>	<b>&lt;0.001</b>	<b>&lt;0.001</b>	<b>&lt;0.001</b>	<b>&lt;0.001</b>	<b>&lt;0.001</b>	<b>&lt;0.001</b>	0.910	0.993	

1-Way ANOVA, unequal var: D/L Ser (F=75.1, df=15.6, p<0.001); D/L Ala (F=242.5, df=15.8, p<0.001)

Notes: Pup/Gly=Pupoides/Glyphalinia; Bonferroni transformation of  $\alpha_{(0.05/46)}=0.00109$

Table 3.6. Pairwise ANOVA for shell condition.

**A:** Tukey's pairwise ***p-val*** by shell condition D/L Asp (upper right); D/L Glu (lower left).

	SC=4	SC=3	SC=2	SC=1
SC=4	1	0.822	<0.001	<0.001
SC=3	0.911	1	<0.001	<0.001
SC=2	<0.001	<0.001	1	0.611
SC=1	<0.001	<0.001	0.617	1

1-way ANOVA, unequal var: D/L Asp (F=89.8, df=3.96, p<0.001); D/L Glu (F=94.9, df=4.33, p<0.001)

**B:** Tukey's pairwise ***p-val*** by shell condition D/L Ser (upper right); D/L Ala (lower left).

	SC=4	SC=3	SC=2	SC=1
SC=4	1	0.076	<0.001	<0.001
SC=3	0.357	1	<0.001	<0.001
SC=2	<0.001	0.001	1	0.992
SC=1	<0.001	<0.001	0.814	1

1-way ANOVA, unequal var: D/L Ser (F=192, df=4.18, p<0.001); D/L Ala (F=123, df=4.68, p<0.001)

Table 3.7. Radiocarbon results from Kulas Quarry and Big Platte.

<b>Sample Loc</b>	<b>Lab#</b>	<b><sup>14</sup>C Age</b>	<b>Cal Age</b>	<b>Depth (m)</b>	<b><i>p-val</i></b>
KQ-15	Beta-223641	16,670±60	19,929±295	2.75	
KQ-15 <sup>a</sup>	AA-83090	16,840±120	20,059±296	2.75	T=12.61,
KQ-15 <sup>a</sup>	AA-83091	17,180±130	20,617±330	2.75	<i>0.0056<sup>b</sup></i>
KQ-15 <sup>a</sup>	AA-83092	16,890±120	20,122±288	2.75	
KQ-05	Beta-223642	17,550±70	20,961±314	4.5	T=4.31,
KQ-05**	AA-82558	17,990±200	21,673±448	4.5	<i>0.038</i>
BP-C1a	Beta-223638	15,710±60	18,964±228	0.15-0.45	
BP-C1a	Beta-223637	15,890±50	19,075±215	0.15-0.45	T=4.2,
BP-C1b	Beta-231781	15,800±100	19,021±229	0.7	<i>0.069</i>
					Tot: T=107, <i>p</i> <<0.0001

Notes: **Depth (m)** indicates below top of section, all dates obtained via AMS <sup>14</sup>C analysis of gastropod shell carbonate. <sup>a</sup>Additional Kulas Quarry dates analyzed by Rech et al. (in prep). **Cal Age** = Calibrated age (cal yr. BP). **T**-statistic based on chi-square distribution of similarity in radiocarbon ages. <sup>a</sup>Probability of same age for KQ-15 improves to *p*=0.122 if Beta 14C sample omitted.



Table 3.8. Descriptive statistics for variables used in PCA. Variables represent AAR results for all succineid shells from Big Platte (*Succinea* cf. *bakeri*) and Kulas Quarry (*Catinella* cf. *gelida*). Results in bold to highlight non-normal data distributions. Refer to Table 3.4 for other summary statistics.

Variable	Big Platte (n=127)		Kulas Quarry (n=55)	
	skew	kurt	skew	kurt
Depth	0.86	-0.02	0.45	-0.79
[Sum]	0.82	3.45	-0.40	0.46
D/L Asp	0.03	-0.04	0.18	-0.47
D/L Glu	0.11	0.05	<b>2.26</b>	<b>8.20</b>
D/L Ser	-0.84	0.82	-0.35	1.33
D/L Ala	<b>2.26</b>	<b>6.34</b>	<b>1.26</b>	<b>2.45</b>
L-Ser/(D+L Asp)	0.74	0.41	0.91	0.30
L-Ser/(D+L Glu)	1.00	0.94	<b>1.03</b>	<b>2.07</b>

Notes: Skewness/Kurtosis values calculated for screened data from succineid shell AAR analyses. Kulas Quarry (*Catinella*) and Big Platte (*Succinea*). Values > 1 in bold to highlight non-normal variables. For data mean & variance, see Table 3.4.

Table 3.9. Eigenvalues from PCA of Big Platte and Kulas Quarry Data.

<b>P.C.</b>	<b>Big Platte</b>			<b>Kulas Quarry</b>		
	<b>E.V.</b>	<b>%Var</b>	<b>B.S.</b>	<b>E.V.</b>	<b>%Var</b>	<b>B.S.</b>
<b>1</b>	<b>3.218</b>	<b>40.2</b> <i>40.2</i>	<b>2.718</b> <i>p=0.001</i>	<b>3.011</b>	<b>37.6</b> <i>37.6</i>	<b>2.718</b> <i>p=0.001</i>
<b>2</b>	<b>1.449</b>	<b>18.1</b> <i>58.3</i>	<b>1.718</b> <i>p=0.001</i>	<b>1.947</b>	<b>24.3</b> <i>61.9</i>	<b>1.718</b> <i>p=0.001</i>
<b>3</b>	<b>1.078</b>	<b>13.5</b> <i>71.8</i>	<b>1.218</b> <i>p=0.879</i>	<b>1.22</b>	<b>15.3</b> <i>77.2</i>	<b>1.218</b> <i>p=0.286</i>

Notes: **P.C.**=Principal Component; **Eigenval.** = eigenvalue of P.C.; **%Var** = proportion of variance explained by component (cumulative in italics); **B.S.** = "Broken Stick," expected eigenval. from random model - if E.V.>B.S., component can be considered "important" (e.g. Jackson, 1993); **p-value** calculated  $(n+1)/(N+1)$ , where  $n$  is no. of randomizations with an E.V. for that axis  $\geq$  observed and  $N$  is the total no. ( $N=999$ ) of randomizations (Peres-Nato et al., 2005).

Table 3.10. Eigenvectors for variables along the first three PCs. Only the first two PCs are considered significant. Note also that “D+L-Asp” is an abbreviation for L-Ser/(D+L Asp) and “D+L-Glu” is an abbreviation for L-Ser/(D+L Glu).

Var	Big Platte			Kulas Quarry		
	1st PC	2nd PC	3rd PC	1st PC	2nd PC	3rd PC
<b>Depth</b>	-0.09	<b>0.67</b>	<b>-0.32</b>	0.12	<b>0.32</b>	<b>0.68</b>
<b>[Sum]</b>	0.25	<b>0.42</b>	<b>0.41</b>	-0.01	<b>0.42</b>	<b>-0.60</b>
<b>D/L-Asp</b>	<b>0.34</b>	<b>0.33</b>	<b>0.35</b>	<b>0.42</b>	-0.11	-0.17
<b>D/L-Glu</b>	<b>0.33</b>	<b>-0.37</b>	<b>0.41</b>	0.25	<b>-0.55</b>	0.20
<b>D/L-Ser</b>	<b>0.48</b>	0.00	-0.29	<b>0.48</b>	0.12	-0.24
<b>D/L-Ala</b>	0.17	<b>-0.31</b>	<b>-0.44</b>	0.23	<b>-0.52</b>	-0.20
<b>D+L-Asp</b>	<b>-0.50</b>	0.11	-0.01	<b>-0.50</b>	-0.14	-0.09
<b>D+L-Glu</b>	<b>-0.44</b>	-0.15	<b>0.40</b>	<b>-0.45</b>	<b>-0.33</b>	-0.11

Note: Eigenvectors (loading) for variables on first three principal components (PCs) at Big Platte and Kulas Quarry. Higher values (+ or -) indicate stronger loading = greater contribution of that variable to the variance along a particular PC. Values  $|EV| \geq 0.30$  are in bold.

Table 3.11. Cross-product matrix for variables from PCA.

Big Platte	Variable	Depth	[Sum]	D/L-Asp	D/L-Glu	D/L-Ser	D/L-Ala	D+L-Asp	D+L-Glu	Kulas Quarry
	Depth	1.00	-0.08	0.03	0.06	0.01	-0.28	-0.27	<b>-0.38</b>	
	[Sum]	0.09	1.00	0.01	<b>-0.48</b>	0.14	0.18	0.01	-0.15	
	D/L-Asp	0.13	<b>0.46</b>	1.00	<b>0.33</b>	<b>0.56</b>	<b>0.36</b>	<b>-0.51</b>	<b>-0.35</b>	
	D/L-Glu	<b>-0.37</b>	0.10	<b>0.32</b>	1.00	0.18	<b>0.63</b>	-0.22	-0.04	
	D/L-Ser	0.00	0.16	<b>0.40</b>	<b>0.45</b>	1.00	0.20	<b>-0.67</b>	<b>-0.69</b>	
	D/L-Ala	-0.15	-0.03	0.05	0.11	0.23	1.00	-0.20	0.00	
	D+L-Asp	0.26	<b>-0.35</b>	<b>-0.44</b>	<b>-0.52</b>	<b>-0.69</b>	-0.28	1.00	<b>0.75</b>	
	D+L-Glu	<b>-0.46</b>	-0.28	-0.03	-0.16	<b>-0.80</b>	-0.16	<b>0.68</b>	1.00	

Notes: numbers indicate correlation coefficients between variables (BP shown lower left, KQ in upper right), higher values (+ or -) indicate stronger correlation. Correlation of a variable and itself is = 1.00. Values of  $|\text{coeff}| \geq 0.30$  in bold.

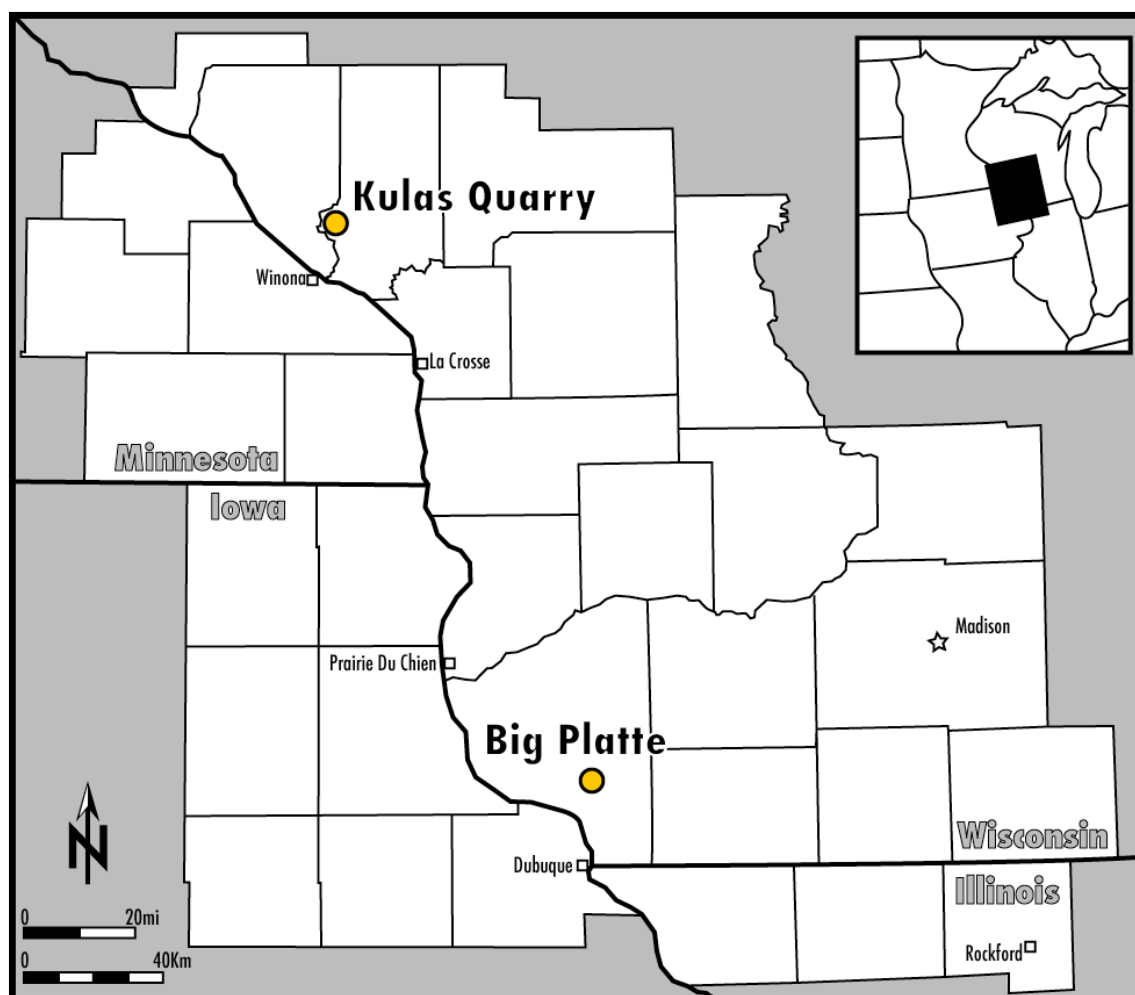


Figure 3.1. Locations of the sites discussed in this chapter.

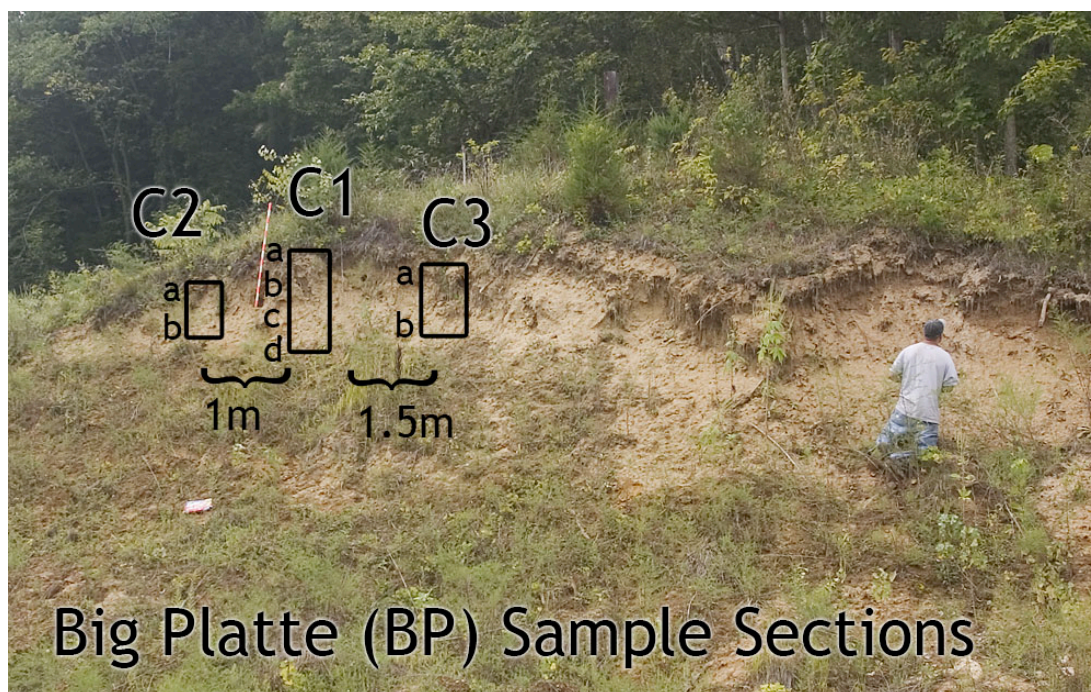


Figure 3.2A Big Platte exposure with locations of samples. Radiocarbon dates obtained from section C1 (See Table 3.8).

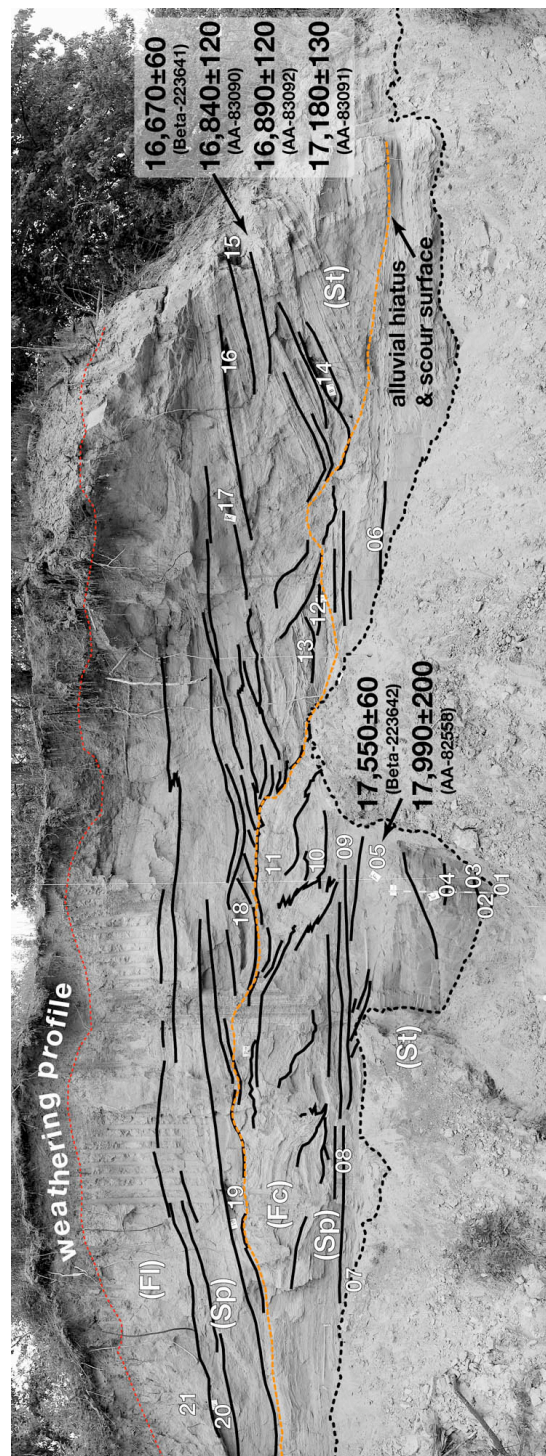


Figure 3.2B. Location of samples from Kulas Quarry. AAR samples obtained from 03, 05, 06, 09, 10, 12, 15, 17, 18, and 20.





Figure 3.3A. Auger sampling at Big Platte.





Figure 3.3B. Selective sampling at Kulas Quarry. Note large cross beds.



Figure 3.3C. Landowner using front-end loader to remove the lower 2 m of cover at Kulas Quarry.



Figure 3.4. Representative photographs of snail taxa analyzed with AAR. Note difference in appearance between Cordilleran-Boreal and Eastern Deciduous Forest Taxa (Table 3.1).

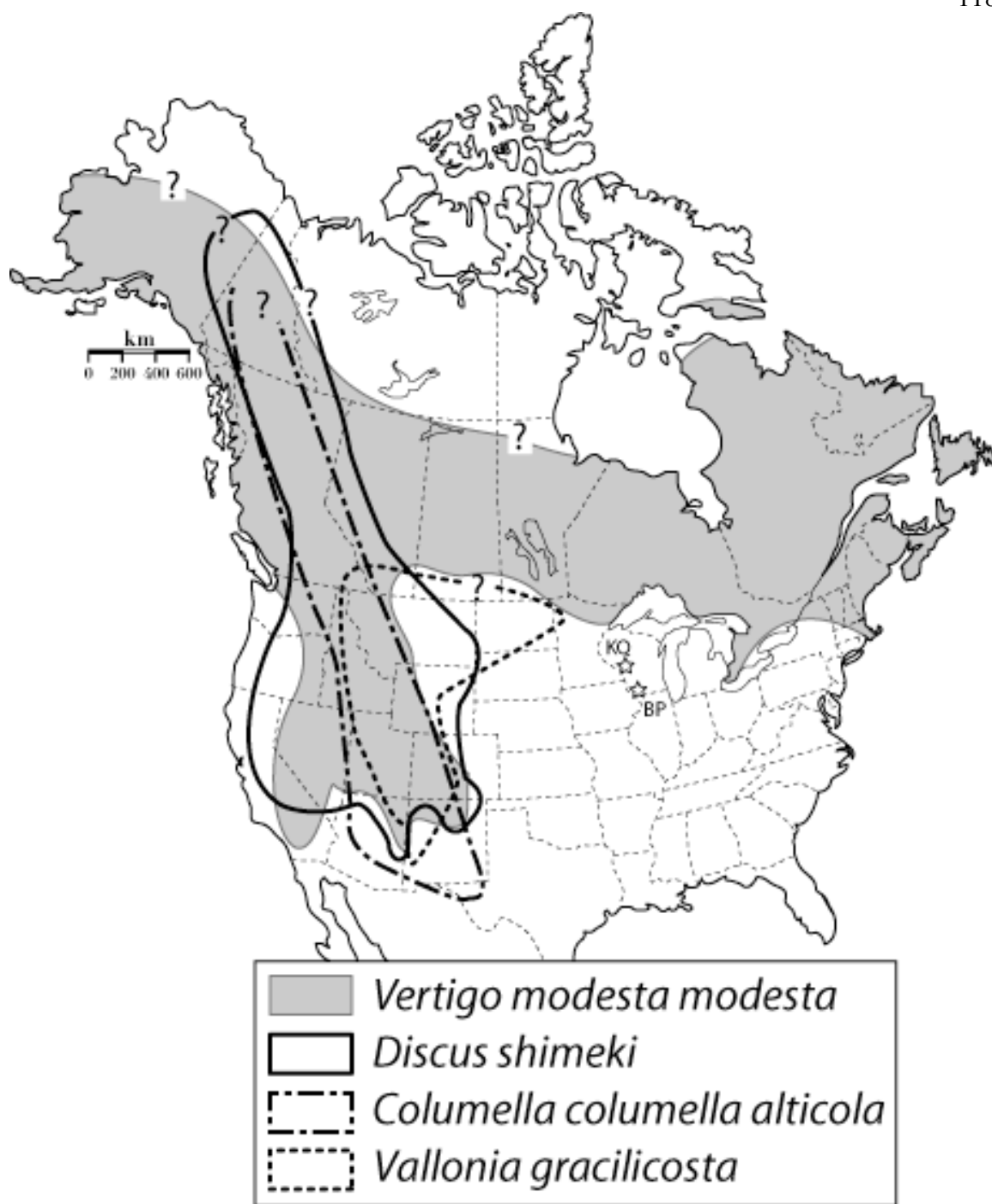


Figure 3.5A. Cordilleran-Boreal gastropod distributions. KQ = Kulas Quarry, BP = Big Platte.



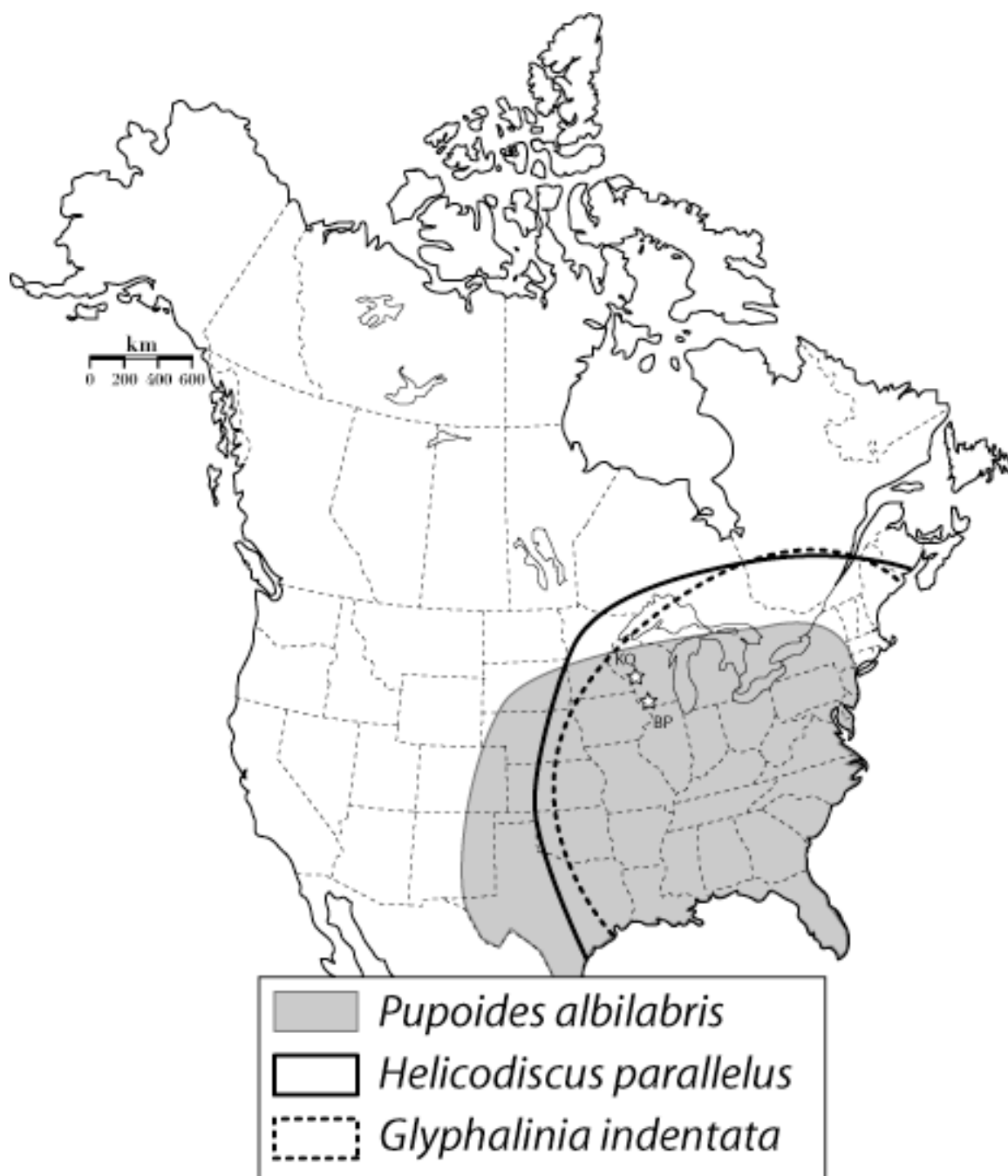


Figure 3.5B. Approximate distributions of selected Eastern Deciduous Forest taxa (data from Hubricht, 1985).

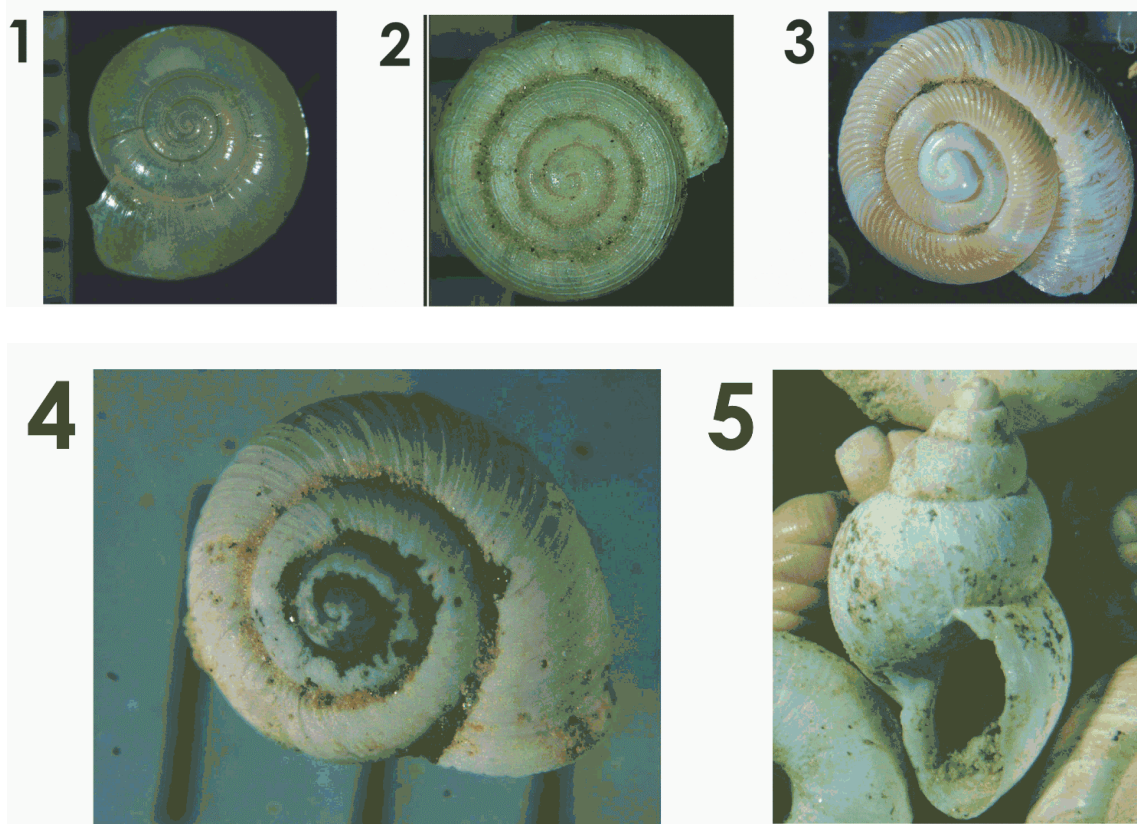


Figure 3.6. Qualitative scale used to score the condition of gastropod shells. 1: *Glyphalinia indentata*, 2: *Helicodiscus parallelus*, 3: *Discus shimeki*, 4: *Vallonia gracilicosta*, 5: *Fossaria* sp.. Note: “5” represents a freshwater gastropod not found at Big Platte.

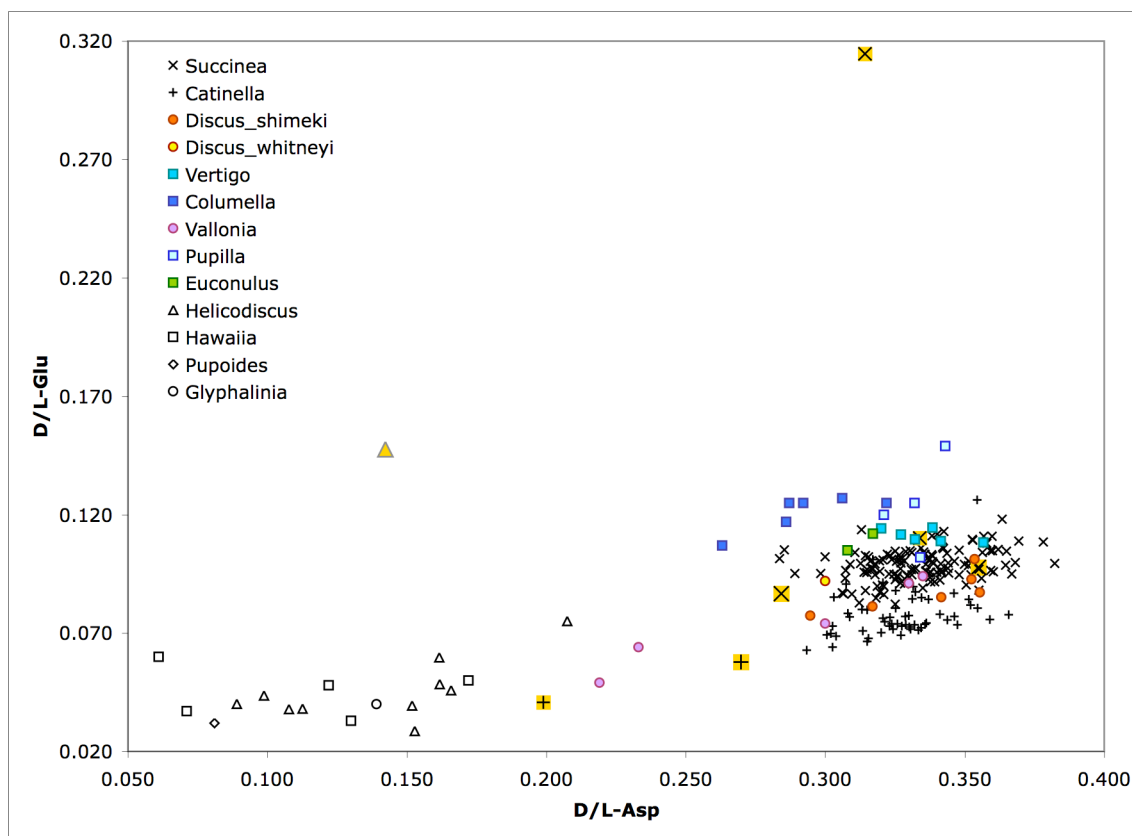


Figure 3.7. D/L Asp and D/L Glu values for all shells. Outliers rejected by data screening are larger and highlighted in yellow. “Younger” Eastern Deciduous Forest Species are represented by open symbols.

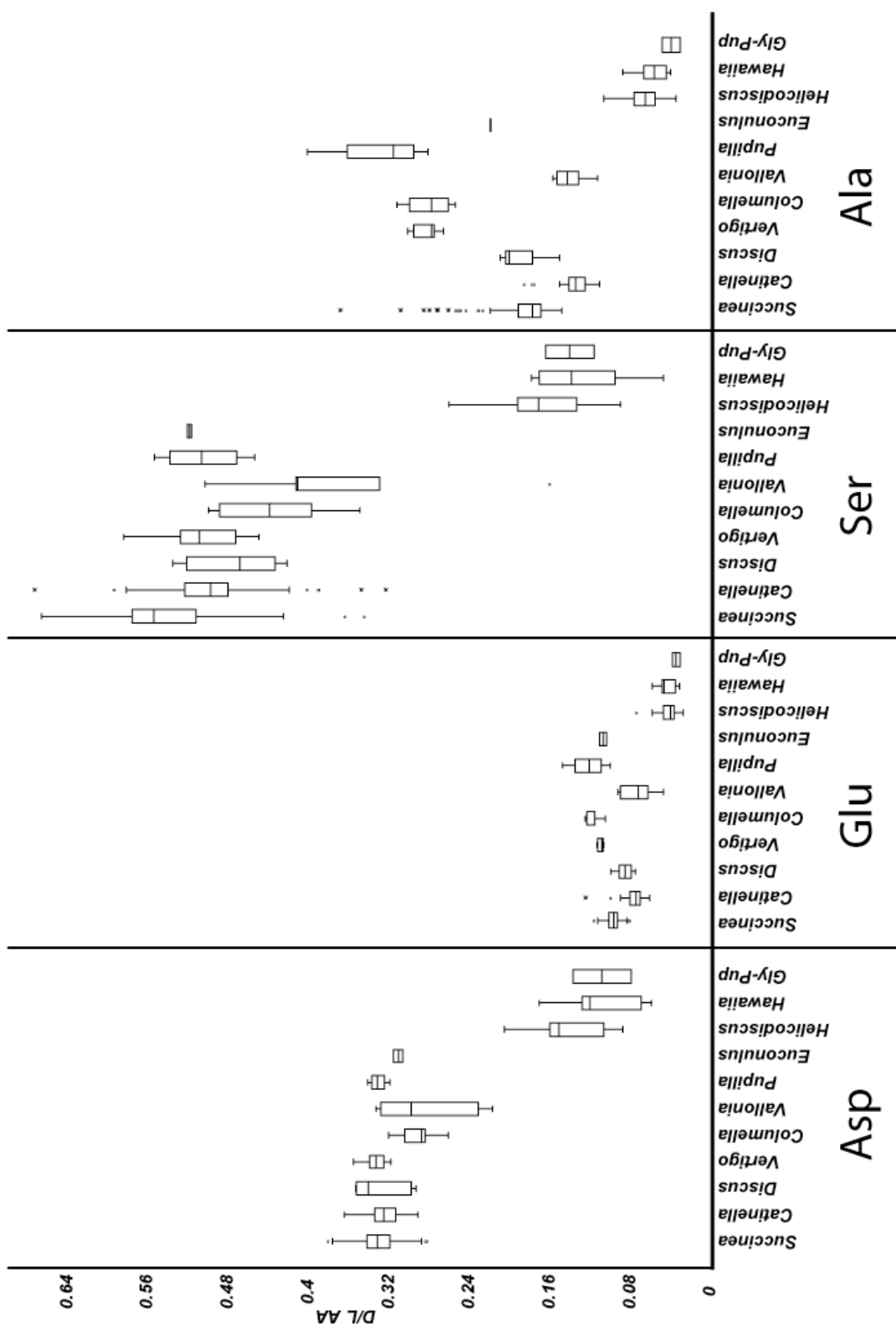


Figure 3.8A. D/L values by taxon. Note: “Gly-Pup” represents combined individual scores from *Glyphalinia* and *Pupoides* shells.



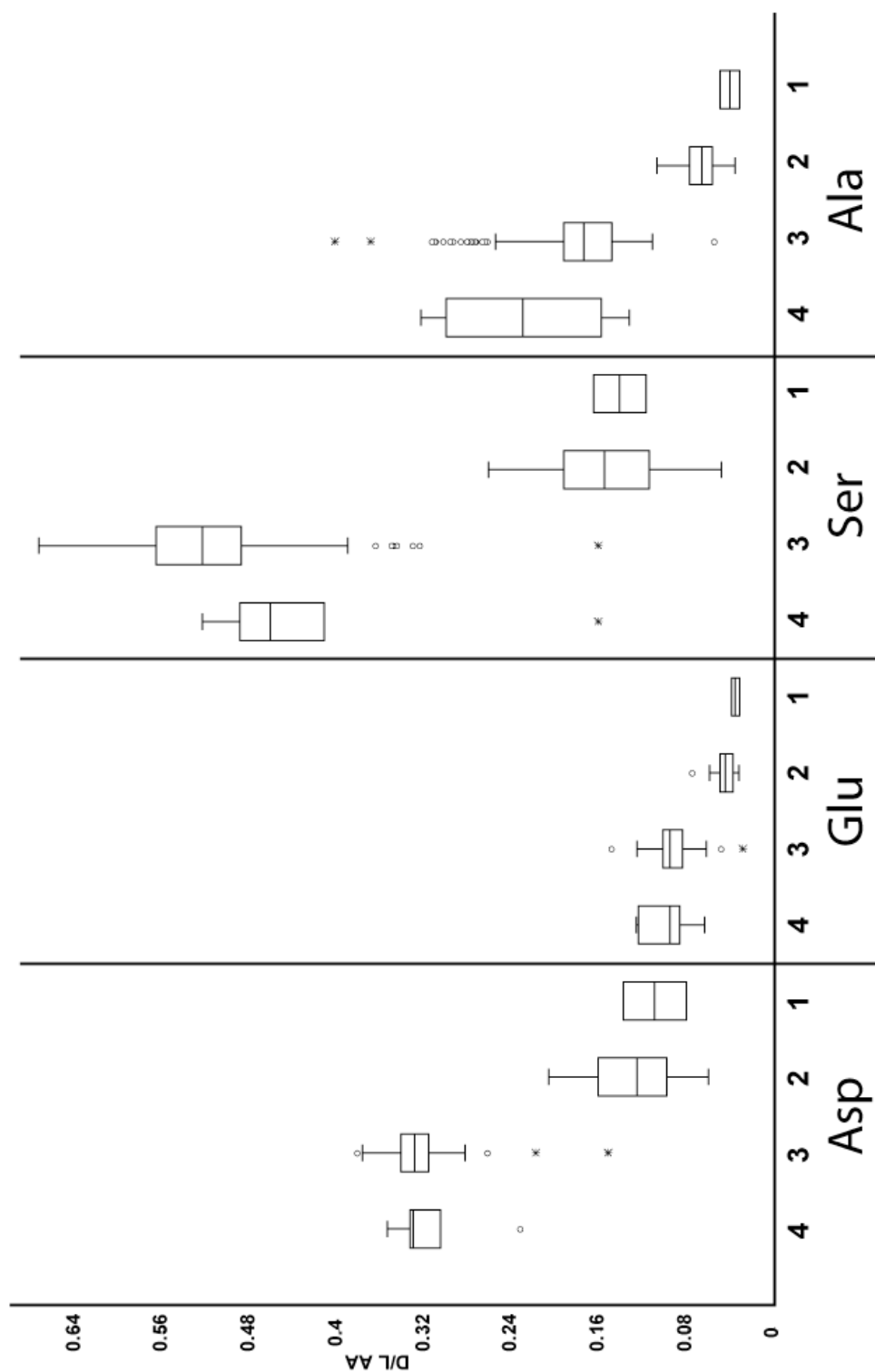


Figure 3.8B. D/L values by shell condition (See Figure 3.6). Note shells with lower condition scores (1 and 2) have lower D/L values for all amino acids compared to shells with higher scores (3 and 4).

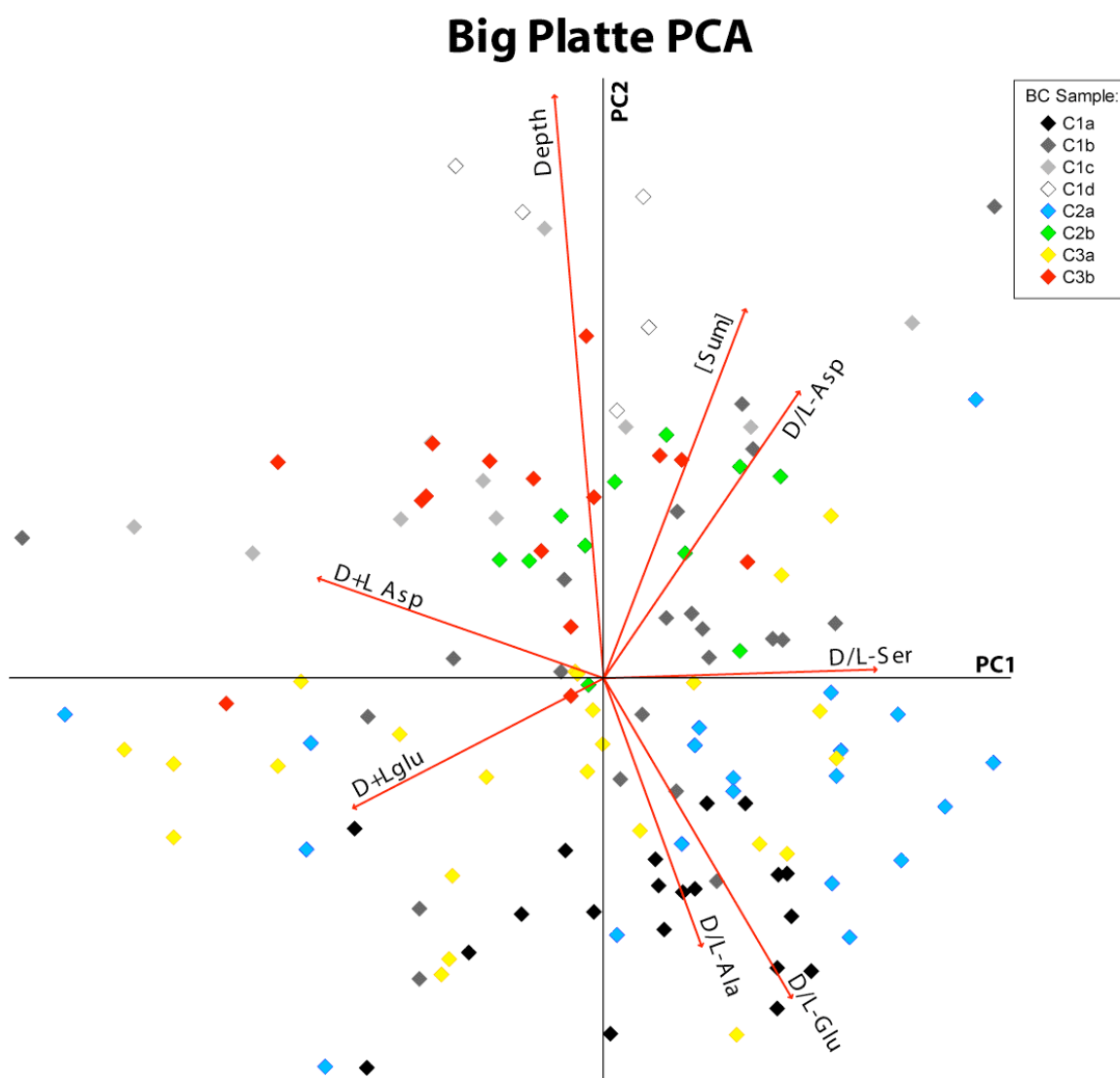


Figure 3.9. Big Platte PCA ordination diagram. Red vectors represent scaled plots of each variable with the length and direction corresponding to the contribution of that variable to each component. Note widely dispersed values for samples from higher in section (C1a, C2a, C3a), which plot lower along PC2 (higher D/L Ala and D/L Glu values).

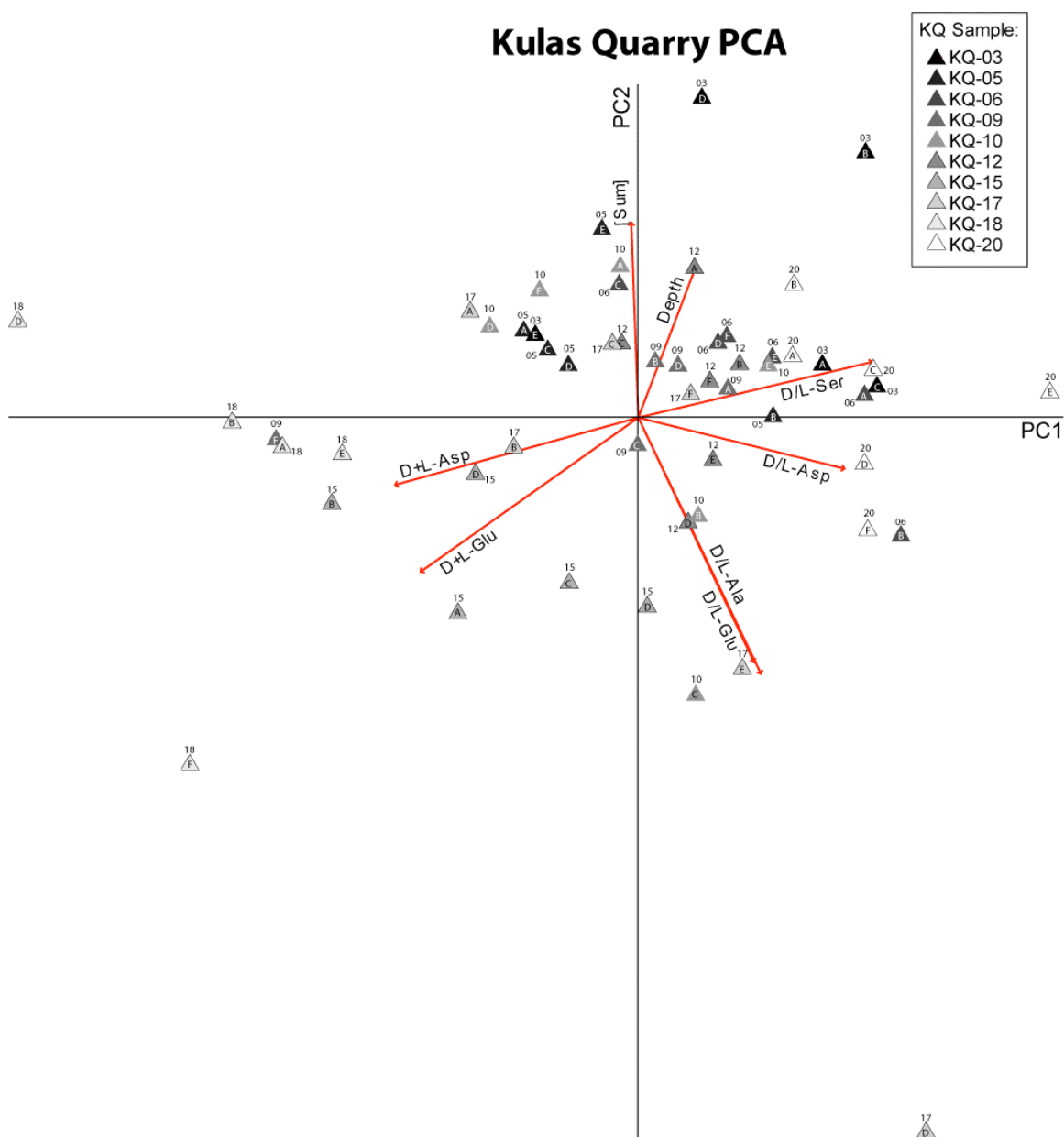


Figure 3.10. Kulas Quarry PCA ordination. Note outliers at left and lower right. Each triangle represents individual shell scores. Letters within triangle correspond to lab# suffix in Appendix A.

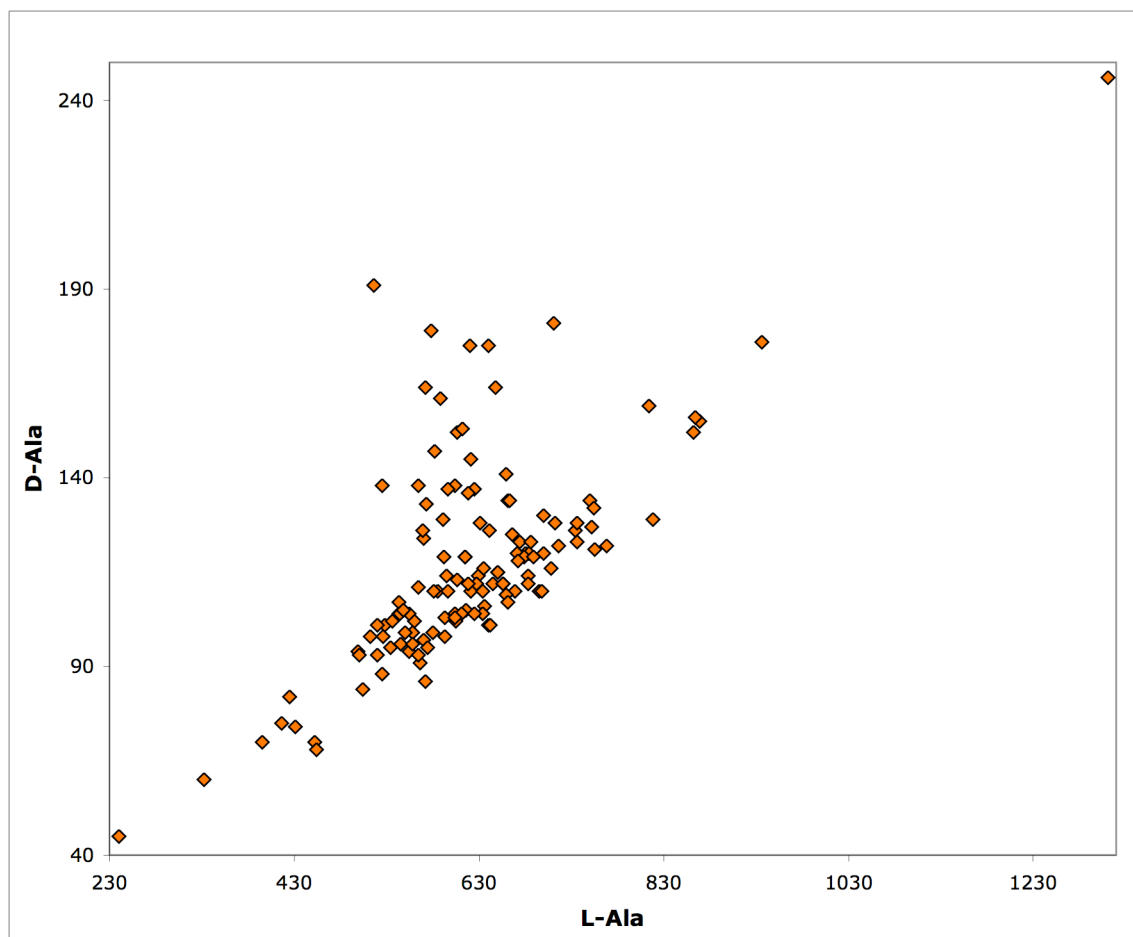


Figure 3.11. Scatterplot of Big Platte *Succinea* AAR data (measured HPLC peak area of L- and D-Ala) showing general linear relationship between D- and L-Ala. The covariance anomaly is represented by higher peak areas of D-Ala relative to L-Ala; although none of these data would appear as a univariate outlier of D-Ala or L-Ala.